Neurobiology of Disease

Loss of the Schizophrenia-Linked Furin Protein from *Drosophila* Mushroom Body Neurons Results in Antipsychotic-Reversible Habituation Deficits

Kyriaki Foka,[1,2] Eirini-Maria Georganta,[1*] Ourania Semelidou,[1*] and Efthimios M. C. Skoulakis[1]
[1]Institute for Fundamental Biomedical Research, Biomedical Science Research Centre "Alexander Fleming," 16672 Vari, Greece, and [2]Department of Molecular Biology and Genetics, Democritus University of Thrace, 68100 Alexandroupolis, Greece

Habituation is a conserved adaptive process essential for incoming information assessment, which drives the behavioral response decrement to recurrent inconsequential stimuli and does not involve sensory adaptation or fatigue. Although the molecular mechanisms underlying the process are not well understood, habituation has been reported to be defective in a number of disorders including schizophrenia. We demonstrate that loss of *furin1*, the *Drosophila* homolog of a gene whose transcriptional downregulation has been linked to schizophrenia, results in defective habituation to recurrent footshocks in mixed sex populations. The deficit is reversible by transgenic expression of the *Drosophila* or human Furin in adult α'/β' mushroom body neurons and by acute oral delivery of the typical antipsychotic haloperidol and the atypical clozapine, which are commonly used to treat schizophrenic patients. The results validate the proposed contribution of Furin downregulation in schizophrenia and suggest that defective footshock habituation is a *Drosophila* protophenotype of the human disorder.

Key words: antipsychotics; *Drosophila*; *furin*; habituation; mushroom bodies; schizophrenia

Significance Statement

Genome-wide association studies have revealed a number of loci linked to schizophrenia, but most have not been verified experimentally in a relevant behavioral task. Habituation deficits constitute a schizophrenia endophenotype. *Drosophila* with attenuated expression of the schizophrenia-linked highly conserved Furin gene present delayed habituation reversible with acute exposure to antipsychotics. This strongly suggests that footshock habituation defects constitute a schizophrenia protophenotype in *Drosophila*. Furthermore, determination of the neurons whose regulated activity is required for footshock habituation provides a facile metazoan system to expediently validate putative schizophrenia genes and variants in a well understood simple brain.

Introduction

Habituation is a highly conserved form of adaptive behavioral plasticity underlying response attenuation to repetitive inconsequential stimuli (Rankin et al., 2009). Mechanistically, processes underlying habituation are thought to drive toward inhibition the excitation/inhibition balance in circuits that process and mediate responses to incoming stimuli (Ramaswami, 2014; Heinze et al., 2021). Habituation latency refers to the time of recurrent stimulation without observable response decrement (Rankin et al., 2009; Semelidou et al., 2018), when processes driving this shift to response inhibition likely occur. Mutations that reduce latency result in premature habituation (Acevedo et al., 2007; Roussou et al., 2019). Conversely, defective habituation may be manifested as prolonged latency or habituation failure, resulting in continued responsiveness to recurrent stimuli (Roussou et al., 2019). Importantly, habituation defects have been associated with a number of neuropsychiatric conditions (McDiarmid et al., 2017; Heinze et al., 2021), including schizophrenia (Meincke et al., 2004; Williams et al., 2013; McDiarmid et al., 2017; Avery et al., 2019).

Schizophrenia is a psychiatric disorder with complex manifestations including hallucinations and delusions (positive symptoms), affective flattening, loss of initiative and anhedonia (negative symptoms), and cognitive deficits in attention,

Received June 1, 2022; revised July 28, 2022; accepted Aug. 7, 2022.
Author contributions: E.M.C.S. designed research; K.F., E.-M.G., and O.S. performed research; K.F., E.-M.G., and O.S. analyzed data; K.F. wrote initial draft; E.M.C.S. wrote the paper.
This research was cofinanced by Greece and the European Union (European Social Fund-ESF) through the Operational Programmes: "Human Resources Development, Education and Lifelong Learning" in the context of the project "Strengthening Human Resources Research Potential via Doctorate Research—2nd Cycle" (MIS-5000432), implemented by the State Scholarships Foundation (IKY) to K.F. and the Hellenic Foundation for Research and Innovation Grant HFRI FM17-TΔE2961 to E.M.C.S. We thank the Bloomington Drosophila Stock Center and Vienna Drosophila Resource Center for stocks, the FlyLight Project Team for images, M. Loizou for technical help, and Dr. I. Maroulakou (Democritus University of Thrace, Alexandroupolis, Greece) for advice.
*E.-M.G. and O.S. contributed equally to this work.
The authors declare no competing financial interests.
Correspondence should be addressed to Efthimios M. C. Skoulakis at skoulakis@fleming.gr.
https://doi.org/10.1523/JNEUROSCI.1055-22.2022

memory, and executive function (van Os and Kapur, 2009; Patel et al., 2014; Christensen and Børglum, 2019). Its etiology is ostensibly complex, with polygenic genetic contributions representing ~80% of the risk to develop the condition (van Os and Kapur, 2009). The concept of endophenotypes was developed to deconvolute the complexity of psychiatric illnesses to fundamental symptoms linked to genetic alterations, which could serve as potential biomarkers (Gottesman and Gould, 2003; Meyer-Lindenberg and Weinberger, 2006; Insel et al., 2010). Much of the genetic evidence comes from genome-wide association studies (GWASs) as disease-associated polymorphisms in multiple loci (Fromer et al., 2016, Richard et al., 2017; Christensen and Børglum, 2019). However, the effect of most schizophrenia-linked polymorphisms on affected or nearby loci has not been experimentally validated, despite studies suggesting association with different manifestations of the condition (Ripke et al., 2014; Richard et al., 2017). Modeling the habituation deficits of schizophrenic patients (Avery et al., 2019) in simple genetically facile experimental organisms has been proposed as necessary to facilitate understanding of the genetic and mechanistic basis of the disease (McDiarmid et al., 2017; Kepler et al., 2020), and this approach is supported by the extensive conservation of schizophrenia risk genes in model organisms (Kasap et al., 2018).

Protophenotypes are endophenotypes conserved in model organisms (Dwyer et al., 2015) and defects in habituation, a process conserved in all species examined (McDiarmid et al., 2017), constitute an accepted schizophrenia endophenotype (Meincke et al., 2004; Avery et al., 2019). Therefore, habituation defects could serve as a protophenotype (Dwyer, 2018) for the disease in *Drosophila*. We have developed habituation paradigms engaging particular neuronal circuits in the *Drosophila* CNS (Acevedo et al., 2007; Semelidou et al., 2018) and a genetic approach to reveal molecular mechanisms underlying latency and habituation (Semelidou et al., 2018; Roussou et al., 2019). The defective habituation of one such mutant was reversed by antipsychotics (Roussou et al., 2019), suggesting that habituation deficits could in principle serve as a schizophrenia-linked protophenotype in *Drosophila*.

To provide support for footshock habituation deficits as a fly schizophrenia protophenotype, we selected *furin*, a gene with polymorphisms strongly associated with the condition (Fromer et al., 2016, Christensen and Børglum, 2019; Schrode et al., 2019) and tested mutants in its *Drosophila* ortholog *furin1* (Roebroek et al., 1993), in this paradigm. Furin is a subtilisin family, calcium-dependent serine endoprotease, which regulates the activity of proprotein substrates including growth factors, receptors, and extracellular-matrix proteins (Thomas, 2002). These Furin substrates are essential for neuronal development in human cultured cells and zebrafish embryos (Fromer et al., 2016). However, the consequences of Furin attenuation ostensibly because of noncoding polymorphisms in the human *furin* gene (Schrode et al., 2019), on neuronal function have not been assessed experimentally. Therefore, *Drosophila* Furin levels were attenuated and its effects on footshock habituation are reported below.

Materials and Methods

Drosophila *husbandry*

Drosophila were raised in standard wheat-flour-sugar food supplemented with soy flour and $CaCl_2$ food (Roussou et al., 2019), at 22–25°C and a 12 h light/dark cycle, unless specified otherwise.

The following strains were obtained from the Bloomington Drosophila Stock Center (BDSC): Furin 1 MiMIC insertion mutants (stock #42180: y^1w^*; Mi[MIC]Fur^{MI06808}; stock #36 401: y^1w^*; Mi[MIC]Fur^{MI03544}, #51 078: y^1w^*; Mi[MIC]Fur^{MI08357}/TM3Sb^1Ser^1 (henceforth $fur1^1$, $fur1^2$, and $fur1^3$, respectively), *furin1* RNA interference [RNAi; stock #42481 and stock #25837, BDSC (henceforth, $fur1^{RNAi1}$ and $fur1^{RNAi2}$)], UAS*furin1* (#63078, BDSC) and UAS*hfurin* (stock #66055, BDSC). All MiMIC mutant strains were normalized to the y^1w^1 (yw) genetic background. To match the genotype of RNAi-expressing flies in driver heterozygotes, all Gal4 driver strains were crossed with the y^1v^1;P(y[+t7.7]=Cary)attP2 (stock #36303, BDSC), which is the genetic background of all RNAi strains used. In the case of $fur1^{RNAi2}$ heterozygotes, the $fur1^{RNAi2}$ strain was crossed with w^{1118} to match the background of the experimental strains it was a control for.

The Gal4 driver strains used have been described before: elav-Gal4 (FlyBase ID: FBrf0237128), MB247-Gal4, dnc-Gal4 (stock #48571, BDSC), c739-Gal4, and c305a-Gal4 (Roussou et al., 2019). The γ neuron driver VT44966-Gal4 (Shyu et al., 2017) was obtained from the Vienna Drosophila Resource Center (stock #203571). The patterns and specificity of the α/β-, α'/β'-, and γ-specific drivers, as well as the pan-MB dncGal4 (FlyLight Project team; Jenett et al., 2012) are seen in Figure 5 by driving UASmyrGFP for the first three and UASmCD8GFP for the last one. Gal80^{ts} was introduced to these driver strains by standard crosses or recombination, as indicated. The following double-transgenic strains were also generated by standard crosses or recombination as necessary: c305a-Gal4; $fur1^1$, VT44966-Gal4, $fur1^1$, UAS*furin1*; $fur1^1$, and UAS*hfurin*, $fur1^1$. UAS-*shibire*^{ts} (Kitamoto, 2001) was used to block neurotransmission. Flies carrying UAS-*shi*^{ts} were raised at 25°C, and the dynamin was inactivated by incubation at 32°C for 30 min before behavioral testing.

Crosses involving strains containing the temperature-sensitive suppressor Gal80^{ts} (TARGET system; McGuire et al., 2004) were raised at 18°C and transferred to 30°C to induce UAS transgene expression for 2 d, as specified, while control flies of the same genotype (uninduced) remained at 18°C for the same amount of time.

Western blots

Five female fly heads at 2–5 d after eclosion were homogenized in 1× Laemmli buffer (50 mM Tris, pH 6.8, 5% 2-mercaptoethanol, 2% SDS, 10% glycerol, and 0.01% bromophenol blue) and loaded per lane. Proteins were transferred to PVDF membrane and probed with the mouse anti-HA-Tag antibody (F-7; catalog #sc-7392, Santa Cruz Biotechnology) at 1:1500. To normalize sample loading, anti-Syntaxin (catalog #mAb 8C3, Developmental Studies Hybridoma Bank) was used at 1:12,000. Mouse HRP-conjugated secondary antibody was applied at 1:5000.

Imaging and immunohistochemistry

The expression patterns and specificity of the dnc-Gal4, c739-Gal4, c305a-Gal4, VT030604-Gal4, and VT44966-Gal4 were revealed by crossing these driver strains to UAS-mCD8GFP reporter strains. To reveal synaptic connections, the trans-TANGO method (Talay et al., 2017) was used by crossing c305a-Gal4, VT030604-Gal4, or VT44966-Gal4 to UASmyrGFP.QUAS-mtdTomato-3xHA (article #77124,) at 25°C and keeping 2- to 3-d-old adults at 30°C for 16–20 h before dissecting brains, staining with appropriate antibodies, and imaging as described before (Georganta et al., 2021). The primary antibodies used were: mouse anti-HA (sc7392, Santa Cruz Biotechnology, 1:400) and rabbit anti-GFP (1:400; catalog #A-6455, Thermo Fisher Scientific). The secondary antibodies were Alexa Fluor 488-conjugated goat anti-mouse and Alexa Fluor 647-conjugated goat anti-rabbit (both were used at 1:400; both from Thermo Fisher Scientific). Fur1 expression images were obtained by permission from the FlyLight Project team (Jenett et al., 2012).

Reverse transcription and PCR

RNA extraction from 30 fly heads of both sexes was performed within 30 min after induction as detailed previously (Kotoula et al., 2017). Detection of transgene-specific transcripts was performed as described

Table 1. Collective statistics

Genotype	Mean ± SEM	*F* ratio	*p*
Figure 1*A*			
ANOVA $F_{(3,43)} = 15.5826$, $p < 0.0001$			
Control (naive)	62.24 ± 3.43	26.599	<0.0001
Control (15 shocks)	37.18 ± 4.16		
fur1^{1} (naive)	64.38 ± 3.35	0.0892	0.7667
fur1^{1} (15 shocks)	65.83 ± 2.64		
Figure 1*B*			
ANOVA $F_{(3,32)} = 4.9721$, $p = 0.0066$			
Control (naive)	67.58 ± 4.55	12.9736	0.0012
Control (15 shocks)	50.20 ± 3.83		
fur1^{2} (naive)	59.08 ± 2.12	1.3794	0.2498
fur1^{2} (15 shocks)	64.91 ± 2.29		
Figure 1*C*			
ANOVA $F_{(5,46)} = 14.553$, $p < 0.0001$			
Control (naive)	53.55 ± 3.40	28.1329	<0.0001
Control (15 shocks)	19.50 ± 4.65		
Control (naive)	53.55 ± 3.40	14.9613	0.0004
Control (30 shocks)	28.72 ± 6.19		
fur1^{1} (naive)	49.45 ± 5.33	2.8797	0.0973
fur1^{1} (15 shocks)	60.72 ± 4.00		
fur1^{1} (naive)	49.45 ± 5.33	17.9564	0.0001
fur1^{1} (30 shocks)	22.24 ± 2.97		
Figure 1*D*			
ANOVA $F_{(5,50)} = 25.4552$, $p < 0.0001$			
Control (naive)	69.93 ± 3.97	82.8	<0.0001
Control (30 shocks)	25.37 ± 5.04		
Control (30 shocks)	25.37 ± 5.04	46.242	<0.0001
Control (30 shocks+YO)	57.73 ± 3.24		
fur1^{1} (naive)	57.61 ± 3	25.847	<0.0001
fur1^{1} (30 shocks)	33.42 ± 1.99		
fur1^{1} (30 shocks)	33.42 ± 1.99	30.458	<0.0001
fur1^{1} (30 shocks+YO)	58.90 ± 2.55		
Figure 1*E*			
ANOVA $F_{(3,47)} = 5.2587$, $p = 0.0035$			
Control (naive)	56.86 ± 4.46	11.388	0.0016
Control (15 shocks)	29.52 ± 5.64		
fur1^{3}/+ (naive)	54.80 ± 7.38	0.0086	0.9267
fur1^{3}/+ (15 shocks)	55.55 ± 5.00		
Figure 1*F*			
ANOVA $F_{(5,41)} = 23.8953$, $p < 0.0001$			
Control (naive)	72.82 ± 4.57	55.6859	<0.0001
Control (30 shocks)	15.45 ± 5.25		
Control (30 shocks)	15.45 ± 5.25	52.186	<0.0001
Control (30 shocks+YO)	71 ± 6.39		
fur1^{3}/+ (naive)	77.04 ± 4.62	43.5035	<0.0001
fur1^{3}/+ (30 shocks)	26.33 ± 6.64		
fur1^{3}/+ (30 shocks)	26.33 ± 6.64	24.4541	<0.0001
fur1^{3}/+ (30 shocks+YO)	64.35 ± 4.77		
Figure 1*G*			
ANOVA $F_{(3,55)} = 0.3457$, $p = 0.7924$			
Control (naive)	54.61 ± 3.42	0.1724	0.6797
Control (6 shocks)	56.43 ± 2.73		
fur1^{1} (naive)	58.79 ± 3.26	0.0445	0.8337
fur1^{1} (6 shocks)	57.87 ± 2.97		
Figure 1*H*			
ANOVA $F_{(3,50)} = 1.4272$, $p = 0.2467$			
Control (naive)	64.60 ± 3.07	2.1592	0.1484
Control (6 shocks)	57.74 ± 3.92		
fur1^{2} (naive)	55.98 ± 3.14	0.0243	0.8769
fur1^{2} (6 shocks)	56.73 ± 3.09		
Figure 1*I*			
ANOVA $F_{(3,54)} = 14.0257$, $p < 0.0001$			
Control (naive)	38.08 ± 5.12	15.9975	0.0002
Control (4 min OCT)	11.05 ± 5.06		

(*Table continues*.)

Table 1 Continued

Genotype	Mean ± SEM	*F* ratio	*p*
fur1^{1} (naive)	52.43 ± 3.19	18.3418	<0.0001
fur1^{1} (4 min OCT)	24.03 ± 5.28		
Figure 1*J*			
ANOVA $F_{(3,47)} = 7.3664$, $p = 0.0004$			
Control (naive)	41.91 ± 5.74	9.4659	0.0036
Control (4 min OCT)	12.85 ± 8.26		
fur1^{2} (naive)	41.37 ± 6.83	12.4708	0.0010
fur1^{2} (4 min OCT)	8.01 ± 5.53		
Figure 2*B*			
MB247-G4,G80^{ts}>*fur1*$^{RNA/1}$			
ANOVA $F_{(3,34)} = 16.3363$, $p < 0.0001$			
UN (naive)	70.25 ± 4.43	34.0487	<0.0001
UN (15 shocks)	30.50 ± 7.83		
IN (naive)	70.48 ± 2.63	0.0346	0.8537
IN (15 shocks)	69.25 ± 3.21		
Figure 2*C*			
c739-G4,G80^{ts}>*fur1*$^{RNA/2}$			
ANOVA $F_{(3,29)} = 7.911$, $p = 0.0007$			
UN (naive)	68.09 ± 3.48	7.9184	0.0092
UN (15 shocks)	47.83 ± 7.58		
IN (naive)	64.37 ± 4.88	14.1932	0.0009
IN (15 shocks)	39.00 ± 2.85		
Figure 2*D*			
c305a-G4;G80^{ts}>*fur1*$^{RNA/1}$			
ANOVA $F_{(3,41)} = 7.2492$, $p = 0.0006$			
UN (naive)	79.53 ± 6.29	18.8628	0.0001
UN (15 shocks)	46.33 ± 6.73		
IN (naive)	72.55 ± 3.72	2.2745	0.1398
IN (15 shocks)	61.56 ± 4.20		
Figure 2*E*			
c305a-G4;G80^{ts}>*fur1*$^{RNA/2}$			
ANOVA $F_{(3,55)} = 5.0754$, $p = 0.0037$			
UN (naive)	82.11 ± 1.86	9.9442	0.0027
UN (15 shocks)	65.82 ± 3.35		
IN (naive)	64.96 ± 4.75	0.0672	0.7964
IN (15 shocks)	66.30 ± 4.01		
Figure 2*F*			
G80^{ts};VT44966-G4>*fur1*$^{RNA/2}$			
ANOVA $F_{(3,45)} = 10.6144$, $p < 0.0001$			
UN (naive)	59.43 ± 3.60	26.993	<0.0001
UN (15 shocks)	32.28 ± 4.12		
IN (naive)	54.30 ± 3.81	0.002	0.9642
IN (15 shocks)	54.05 ± 3.47		
Figure 2*G*			
VT44966-G4>UAS*shi*^{ts}			
ANOVA $F_{(5,79)} = 5.1596$, $p = 0.0004$			
+>UAS*shi*^{ts} (naive)	60.43 ± 4.57	11.9565	0.0009
+>UAS*shi*^{ts} (15 shocks)	41.07 ± 4.26		
VT44966-G4>+ (naive)	61.35 ± 4.44	7.8998	0.0063
VT44966-G4>+ (15 shocks)	46.74 ± 3.25		
VT44966-G4>UAS*shi*^{ts} (naive)	61.92 ± 4.15	0.7594	0.3863
VT44966-G4>UAS*shi*^{ts} (15 shocks)	56.84 ± 2.10		
Figure 2*H*			
dnc-G4,G80^{ts}>+			
ANOVA $F_{(3,43)} = 23.7752$, $p < 0.0001$			
UN (naive)	65.68 ± 5.15	34.9817	<0.0001
UN (15 shocks)	27.17 ± 4.18		
IN (naive)	65.01 ± 4.95	36.2933	<0.0001
IN (15 shocks)	25.77 ± 4.04		
Figure 2*I*			
c305a-G4;G80^{ts}>+			
ANOVA $F_{(3,45)} = 11.82$, $p < 0.0001$			
UN (naive)	60.41 ± 4.37	15.882	0.0003
UN (15 shocks)	25.20 ± 10.83		

(*Table continues*.)

Table 1 Continued

Genotype	Mean ± SEM	*F* ratio	*p*
IN (naive)	56.77 ± 4.14	18.3999	0.0001
IN (15 shocks)	22.37 ± 4.82		
Figure 2*J*			
G80^{ts};VT44966-G4>+			
ANOVA $F_{(3,34)} = 43.7431$, $p < 0.0001$			
UN (naive)	66.19 ± 3.74	57.0926	<0.0001
UN (15 shocks)	19.53 ± 4.79		
IN (naive)	67.55 ± 2.85	74.078	<0.0001
IN (15 shocks)	18.71 ± 4.8		
Figure 3*C*			
c305a-G4/UAS*fur1*; *fur1*^{1}/*fur1*^{1}			
1 d induction			
ANOVA $F_{(7,83)} = 5.7847$, $p < 0.0001$			
fur1^{1} (naive)	48.97 ± 4.48	1.8153	0.1819
fur1^{1} (15 shocks)	39.74 ± 5.03		
c305a-G4/+; *fur1*^{1}/+ (naive)	54.00 ± 3.63	10.2535	0.002
c305a-G4/+; *fur1*^{1}/+ (15 shocks)	34.28 ± 2.56		
UAS*fur1*/+; *fur1*^{1}/+ (naive)	50.56 ± 5.66	16.9432	<0.0001
UAS*fur1*/+; *fur1*^{1}/+ (15 shocks)	25.75 ± 5.13		
c305a-G4/UAS*fur1*; *fur1*^{1}/*fur1*^{1} (naive)	53.15 ± 3.08	7.9254	0.0062
c305a-G4/UAS*fur1*; *fur1*^{1}/*fur1*^{1} (15 shocks)	35.39 ± 4.98		
Figure 3*D*			
c305a-G4/+; UAS*hfur*, *fur1*^{1}/*fur1*^{1}			
1 d induction			
ANOVA $F_{(7,64)} = 19.4922$, $p < 0.0001$			
fur1^{1} (naive)	46.61 ± 2.55	0.1676	0.6838
fur1^{1} (15 shocks)	44.41 ± 3.45		
c305a-G4/+; *fur1*^{1}/+ (naive)	63.09 ± 2.69	36.4826	<0.0001
c305a-G4/+; *fur1*^{1}/+ (15 shocks)	33.57 ± 4.02		
UAS*hfur*, *fur1*^{1}/+ (naive)	80.10 ± 2.08	19.6632	<0.0001
UAS*hfur*, *fur1*^{1}/+ (15 shocks)	56.31 ± 4.23		
c305a-G4/+; UAS*hfur*, *fur1*^{1}/*fur1*^{1} (naive)	67.10 ± 4.01	38.8837	<0.0001
c305a-G4/+; UAS*hfur*, *fur1*^{1}/*fur1*^{1} (15 shocks)	35.70 ± 4.55		
Figure 3*G*			
UAS*fur1*/+; VT44966-G4, *fur1*^{1}/*fur1*^{1}			
1 d induction			
ANOVA $F_{(7,75)} = 8.0094$, $p < 0.0001$			
fur1^{1} (naive)	53.52 ± 6.84	0.0348	0.8525
fur1^{1} (15 shocks)	52.09 ± 5.45		
VT44966-G4, *fur1*^{1}/+ (naive)	68.84 ± 4.30	24.445	<0.0001
VT44966-G4, *fur1*^{1}/+ (15 shocks)	32.75 ± 5.32		
UAS*fur1*/+; *fur1*^{1}/+ (naive)	68.95 ± 4.49	13.1299	0.0006
UAS*fur1*/+; *fur1*^{1}/+ (15 shocks)	42.51 ± 6.72		
UAS*fur1*/+; VT44966-G4, *fur1*^{1}/*fur1*^{1} (naive)	61.34 ± 5.31	4.1821	0.0447
UAS*fur1*/+; VT44966-G4, *fur1*^{1}/*fur1*^{1} (15 shocks)	77.07 ± 2.58		
Figure 3*H*			
VT44966-G4, *fur1*^{1}/UAS*hfur*, *fur1*^{1}			
1 d induction			
ANOVA $F_{(7,55)} = 9.3652$, $p < 0.0001$			
fur1^{1} (naive)	53.87 ± 6.28	0.5697	0.4541
fur1^{1} (15 shocks)	58.33 ± 4.62		
VT44966-G4, *fur1*^{1}/+ (naive)	73.17 ± 2.66	14.6014	0.0004
VT44966-G4, *fur1*^{1}/+ (15 shocks)	48.05 ± 3.31		
UAS*hfur*, *fur1*^{1}/+ (naive)	75.93 ± 2.40	23.1313	<0.0001
UAS*hfur*, *fur1*^{1}/+ (15 shocks)	44.31 ± 6.17		
VT44966-G4, *fur1*^{1}/UAS*hfur*, *fur1*^{1} (naive)	77.50 ± 3.53	0.0122	0.9124
VT44966-G4, *fur1*^{1}/UAS*hfur*, *fur1*^{1} (15 shocks)	76.80 ± 2.98		
Figure 3*J*			
c305a-G4/+; *fur1*^{1}/*fur1*^{1}			
1 d induction			

(*Table continues*.)

Table 1 Continued

Genotype	Mean ± SEM	*F* ratio	*p*
ANOVA $F_{(5,55)} = 6.8503$, $p < 0.0001$			
fur1^{1} (naive)	42.66 ± 2.76	0.3879	0.5362
fur1^{1} (15 shocks)	47.44 ± 4.53		
c305a-G4/+; *fur1*^{1}/*fur1*^{1} (naive)	60.57 ± 6.46	0.087	0.7692
c305a-G4/+; *fur1*^{1}/*fur1*^{1} (15 shocks)	62.59 ± 5.59		
c305a-G4/+; *fur1*^{1}/+ (naive)	61.74 ± 4.4	20.0779	<0.0001
c305a-G4/+; *fur1*^{1}/+ (15 shocks)	31 ± 4.55		
Figure 4*A*			
c305a-G4;G80^{ts}>*fur1*^{RNAi2}			
ANOVA $F_{(9,111)} = 3.3112$, $p = 0.0014$			
UN vehicle (naive)	84.85 ± 3.09	10.945	0.0013
UN vehicle (15 shocks)	61.82 ± 4.75		
IN vehicle (naive)	62.37 ± 6.23	0.4499	0.5039
IN vehicle (15 shocks)	67.05 ± 5.31		
IN 2 nM haloperidol (naive)	66.84 ± 5.90	1.8443	0.1774
IN 2 nM haloperidol (15 shocks)	57.58 ± 2.76		
IN 5 nM haloperidol (naive)	64.96 ± 5.52	1.3897	0.2412
IN 5 nM haloperidol (15 shocks)	56.75 ± 3.82		
IN 10 nM haloperidol (naive)	76.95 ± 4.03	7.1572	0.0087
IN 10 nM haloperidol (15 shocks)	58.71 ± 5.60		
Figure 4*B*			
c305a-G4;G80^{ts}>*fur1*^{RNAi2}			
ANOVA $F_{(9,113)} = 2.6165$, $p = 0.0091$			
UN vehicle (naive)	65.97 ± 3.53	7.8718	0.0060
UN vehicle (15 shocks)	43.90 ± 5.02		
IN vehicle (naive)	36.93 ± 8.0	4.1183	0.0450
IN vehicle (15 shocks)	53.57 ± 4.76		
IN 2 nM risperidone (naive)	37.21 ± 4.68	0.0001	0.9909
IN 2 nM risperidone (15 shocks)	37.31 ± 3.12		
IN 5 nM risperidone (naive)	41.31 ± 5.76	0.0872	0.7684
IN 5 nM risperidone (15 shocks)	43.78 ± 7.42		
IN 10 nM risperidone (naive)	36.73 ± 7.24	1.2422	0.2676
IN 10 nM risperidone (15 shocks)	46.07 ± 6.52		
Figure 4*C*			
c305a-G4;G80^{ts}>*fur1*^{RNAi2}			
ANOVA $F_{(9,110)} = 2.9796$, $p = 0.0035$			
UN vehicle (naive)	79.07 ± 3.81	10.391	0.0017
UN vehicle (15 shocks)	59.44 ± 5.39		
IN vehicle (naive)	58.06 ± 6.57	0.0507	0.8222
IN vehicle (15 shocks)	59.55 ± 5.49		
IN 2 nM clozapine (naive)	72.80 ± 4.83	9.1488	0.0032
IN 2 nM clozapine (15 shocks)	52.27 ± 4.27		
IN 5 nM clozapine (naive)	68.31 ± 3.23	0.7165	0.3993
IN 5 nM clozapine (15 shocks)	62.40 ± 3.07		
IN 10 nM clozapine (naive)	61.48 ± 4.61	0.0147	0.9038
IN 10 nM clozapine (15 shocks)	60.68 ± 3.20		
Figure 4*D*			
c305a-G4;G80^{ts}>*fur1*^{RNAi2}			
ANOVA $F_{(5,60)} = 5.979$, $p = 0.0002$			
UN vehicle (naive)	61.10 ± 3.82	7.1849	0.0097
UN vehicle (15 shocks)	44.90 ± 4.76		
IN vehicle (naive)	45.81 ± 3.71	1.4547	0.2329
IN vehicle (15 shocks)	53.56 ± 4.40		
IN 1 nM clozapine (naive)	62.67 ± 4.56	19.9331	<0.0001
IN 1 nM clozapine (15 shocks)	35.69 ± 4.36		
Figure 4*E*			
+>*fur1*^{RNAi2}			
ANOVA $F_{(7,87)} = 8.124$, $p < 0.0001$			
UN vehicle (naive)	55.55 ± 4.94	10.9421	0.0014
UN vehicle (15 shocks)	29.11 ± 5.85		
UN 10 nM haloperidol (naive)	55.96 ± 5.17	8.0298	0.0058
UN 10 nM haloperidol (15 shocks)	33.31 ± 7.38		
IN vehicle (naive)	58.09 ± 5.87	15.9516	0.0001
IN vehicle (15 shocks)	26.17 ± 4.84		

(*Table continues*.)

Table 1 Continued

Genotype	Mean ± SEM	*F* ratio	*p*
IN 10 nM haloperidol (naive)	51.43 ± 6.16	18.1904	<0.0001
IN 10 nM haloperidol (15 shocks)	17.34 ± 4.47		
Figure 4*F*			
+>*fur1*^{RNAi2}			
ANOVA $F_{(7,87)} = 3.7428$, $p = 0.0015$			
UN vehicle (naive)	55.55 ± 4.94	9.9875	0.0022
UN vehicle (15 shocks)	29.11 ± 5.85		
UN 2 nM clozapine (naive)	48.62 ± 5.91	0.0472	0.8286
UN 2 nM clozapine (15 shocks)	46.8 ± 7.13		
IN vehicle (naive)	58.09 ± 5.87	14.56	0.0003
IN vehicle (15 shocks)	26.17 ± 4.84		
IN 2 nM clozapine (naive)	40.91 ± 6.12	0.0009	0.9767
IN 2 nM clozapine (15 shocks)	40.66 ± 6.35		
Figure 4*G*			
G80^{ts};VT44966-G4>*fur1*^{RNAi2}			
ANOVA $F_{(9,86)} = 6.7678$, $p < 0.0001$			
UN vehicle (naive)	72.04 ± 3.76	9.6549	0.0026
UN vehicle (15 shocks)	54.83 ± 3.35		
IN vehicle (naive)	45.01 ± 4.05	0.0382	0.8456
IN vehicle (15 shocks)	46.17 ± 5.42		
IN 2 nM clozapine (naive)	60.72 ± 4.55	0.1411	0.7082
IN 2 nM clozapine (15 shocks)	58.34 ± 4.98		
IN 2 nM risperidone (naive)	59.42 ± 5.00	0.1604	0.6899
IN 2 nM risperidone (15 shocks)	56.89 ± 3.48		
IN 2 nM haloperidol (naive)	71.32 ± 2.82	30.2152	<0.0001
IN 2 nM haloperidol (15 shocks)	36.47 ± 5.19		
Figure 4*H*			
dnc-G4,G80^{ts}>*fur1*^{RNAi2}			
ANOVA $F_{(9,143)} = 3.8072$, $p = 0.0003$			
UN vehicle (naive)	73.88 ± 3.49	12.7352	0.0005
UN vehicle (15 shocks)	50.50 ± 4.62		
IN vehicle (naive)	55.79 ± 6.07	2.507	0.1157
IN vehicle (15 shocks)	67.11 ± 3.35		
IN 2 nM clozapine (naive)	61.27 ± 5.00	0.0572	0.8114
IN 2 nM clozapine (15 shocks)	59.65 ± 3.86		
IN 2 nM haloperidol (naive)	59.65 ± 7.04	1.8679	0.174
IN 2 nM haloperidol (15 shocks)	50.55 ± 4.69		
IN 10 nM haloperidol (naive)	74.41 ± 2.84	14.4551	0.0002
IN 10 nM haloperidol (15 shocks)	48.15 ± 5.06		

previously (Kotoula et al., 2017). Briefly, transgene-specific transcripts were selected and reverse transcribed with transgene-specific reverse primers, while PCR amplification of the transgene-specific cDNAs was achieved with transgene-specific forward primers in addition to the reverse primers used for reverse transcription (Kotoula et al., 2017).

Behavioral analyses

Crosses for behavioral experiments. For the UAS-*shi*^{ts} crosses, UAS-*shi*^{ts} and Gal4 driver homozygotes were crossed en masse to their cognate genetic control strain *w*^{1118}, to obtain heterozygous controls. For the genetic rescue experiments, female c305a-Gal4; *fur1*^{1} or VT44966-Gal4, *fur1*^{1} were crossed to either UAS*furin1*; *fur1*^{1} or UAS*hfurin*, *fur1*^{1} to obtain the experimental animals. For these experiments, heterozygous controls were used, obtained by crossing the c305a-Gal4; *fur1*^{1} or VT44966-Gal4, *fur1*^{1} and UAS*furin1*; *fur1*^{1} or UAS*hfurin*, *fur1*^{1} animals with *y*^{1}*w*^{1} flies.

To examine whether the temperature shift was responsible for the observed deficient habituation phenotype, driver and *fur1*^{RNAi2} heterozygotes raised at 18°C until hatching and were then separated into two groups. Half of them stayed at 18°C (uninduced) and the other were placed at 30°C (induced) for 2 d before training and testing. The heat induction does not affect habituation to footshocks. To ascertain that the presence of c305a-G4 driver alone does not suffice to rescue the habituation deficit, c305a-Gal4/+; *fur1*^{1}/*fur1*^{1} animals, were raised at 18°C until hatching and then were transferred to 30°C for 1 d before training and testing.

Shock habituation. For the training phase, ~50–70 flies were sequestered in the upper arm of a standard T-maze lined with an electrifiable grid. They were exposed to 1.2 s electric shocks at 45 V with a 5.15 s interstimulus interval. After a 30 s rest and 30 s for transfer to the lower part of the maze, the flies were tested by choosing between an electrified and an inert grid. Testing was performed at the same voltage, shock duration, and interstimulus interval as for training. During the 90 s choice period, 17–18 1.2 s stimuli were delivered to the electrified arm of the maze. At the end of the choice period, the flies in each arm were trapped and counted, and the performance index (PI) was calculated as the percentage of the fraction of flies that avoided the electrified grid, minus the fraction of flies present in the arm with the electrified grid (Acevedo et al., 2007).

Dishabituation. To distinguish habituation from fatigue or sensory adaptation after 30 footshocks, flies were dishabituated post-training with an 8 s puff of yeast odor (YO) carried in air drawn at 500 ml/min over a 30% (w/v) aqueous solution of Brewer's yeast (catalog #68876–77-7, Acros Organics) and then were submitted to testing (Roussou et al., 2019).

Olfactory habituation. The olfactory habituation assay was performed as described previously (Semelidou et al., 2018) using 3-octanol as the aversive odorant. The PI was calculated as the percentage of the fraction of flies that avoided the odorant, minus the fraction of flies that did not and remained in the odor-carrying arm (Semelidou et al., 2018).

Drug treatment details. Clozapine was used at final concentrations of 1 nM, 2 nM, 5 nM, 10 nM, and 10 μM, and risperidone and haloperidol were used at 2 nM, 5 nM, 10 nM, and 10 μM. Flies were exposed to drug or vehicle only containing yeast paste for 14–16 h. The following day, the flies were transferred in normal food vials for 1 h before the behavioral task, trained, and tested. Since flies from both sexes were used, to determine whether the sex of the animals impacted their behavioral output, possibly because of differential yeast paste consumption by the females, mixed-sex +>*fur1*^{RNAi2} populations were treated with vehicle or antipsychotics at the relevant concentrations after standard 2 d induction or uninduced and were trained as mixed populations, but the PI of males and females was calculated separately.

To test the effect of the temperature shift (induction) on the responsiveness to drugs, mixed-sex +>*fur1*^{RNAi2} flies were either maintained at 18°C (uninduced) after hatching or shifted to 30°C (induced) and treated with the concentrations of clozapine and haloperidol that rescued the phenotype.

Experimental design and statistical analyses

For all experiments, controls and genetically matched experimental genotypes were tested in the same session in a balanced experimental design. The order of training and testing was randomized. When two genetic controls were used, we required results from experimental animals to be significantly different from both genetic controls. Untransformed (raw) data were analyzed parametrically with the JMP 9 statistical software package (SAS Institute). If significant, initial ANOVAs were followed by planned comparisons [least square mean (LSM) contrast analyses], as to whether they indicated significant differences among the genotypes and the level of significance was adjusted for the experiment-wise error rate as suggested by Sokal and Rohlf (2012). All statistical comparisons are detailed in the text and the collective statistics table (Table 1).

Results

Furin1 is necessary for habituation to recurrent footshocks within specific adult mushroom body neurons

To determine whether Furin1 (Fur1) activity is required for *Drosophila* footshock habituation, we used two homozygous viable and a lethal transposon insertion allele *fur1*^{1}, *fur1*^{2}, and *fur1*^{3}, respectively (for genotypes, see Materials and Methods).

Both viable allele homozygotes did not habituate after experiencing 15 recurrent stimuli of 45 V DC (Acevedo et al., 2007; Roussou et al., 2019), in contrast to controls (Fig. 1*A*: ANOVA: $F_{(3,43)} = 15.5826$, $p < 0.0001$; subsequent LSM, control naive vs

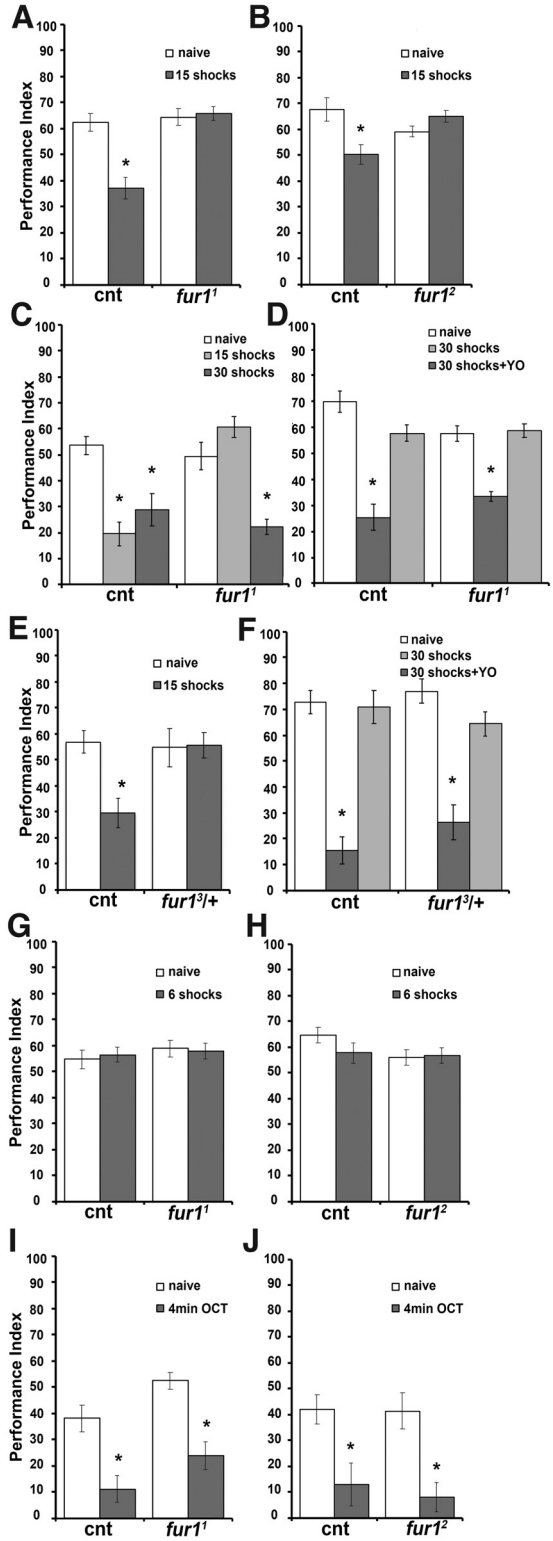

Figure 1. Furin1 is necessary for shock habituation. Mean ± SEM performance indices calculated, as detailed in Materials and Methods, are shown. Values indicate aversion of the shock stimuli and movement toward the stimulus-devoid arm of the maze. Dark gray bars represent the response of control and mutant flies to the test stimuli after pre-experiencing 6, 15, or 30 footshocks or 4 min of 3-octanol. Open bars represent the naive responses to the test stimuli. Light gray bars represent the dishabituation response of control and mutant flies to the test footshock stimuli after pre-experiencing 30 such footshocks and 8 s of yeast odor (YO). Stars indicate significant differences from the naive response, and the collective statistical details are presented in Table 1. ***A***, ***B***, Footshock avoidance of control flies and Furin1 mutants *fur1*^{1} and *fur1*^{2}, either naive or after pre-exposure to 15 shocks: $n \geq 11$ for *fur1*^{1} and $n \geq 8$ for *fur1*^{2}. ***C***, Assessment of the avoidance of control and *fur1*^{1} mutant flies naive or exposed to 15 or 30 shocks: $n \geq 7$ for all groups. ***D***, Footshock avoidance assessment of control and *fur1*^{1} mutant flies, either naive or after exposure to 30 shocks or 30 shocks followed by 8 s of a YO: $n \geq 8$ for all groups. ***E***, Shock avoidance of control and *fur1*^{3}/+ mutant flies exposed to 15 footshocks compared with naïve: $n = 12$ for all groups. ***F***, Footshock avoidance of control and *fur1*^{3}/+ mutants exposed to 30 footshocks or 30 footshocks followed by 8 s of a YO, compared with naïve: $n = 7$ for all groups. ***G***, ***H***, Shock avoidance of control flies and *fur1*^{1} and *fur1*^{2} mutants exposed to six footshocks or naïve: $n = 14$ for *fur1*^{1} and $n \geq 12$ for *fur1*^{2}. ***I***, ***J***, Avoidance assessment of control flies and *fur1*^{1} and *fur1*^{2} mutants after 4 min of exposure to 3-octanol compared with naïve: $n \geq 13$ for *fur1*^{1} and $n \geq 12$ for *fur1*^{2}.

15 shocks, $p < 0.0001$; and *fur1*^{1} naive vs 15 shocks, $p = 0.7667$; Fig. 1*B*: ANOVA: $F_{(3,32)} = 4.9721$, $p = 0.0066$; subsequent LSM: control naive vs 15 shocks, $p = 0.0012$; and *fur1*^{2} naive vs 15 shocks, $p = 0.2498$), which presented a significant post-training reduction in shock avoidance. However, footshock avoidance of the mutants remained within the levels of control animals (Fig. 1*A*,*B*), indicating that Fur1 is not involved in perception or transmission of this aversive stimulus. A similar habituation failure was presented by the *fur1*^{3}/+ animals (Fig. 1*E*: ANOVA: $F_{(3,47)} = 5.2587$, $p = 0.0035$; subsequent LSM: control naive vs 15 shocks, $p = 0.0016$; and *fur1*^{3}/+ naive vs 15 shocks, $p = 0.9267$). To determine whether the observed phenotype results from prolonged latency or actual habituation failure, *fur1*^{1} homozygotes were exposed to 30 footshocks, which, as in similarly treated controls, resulted in emergence of the habituated response (Fig. 1*C*; ANOVA: $F_{(5,46)} = 14.553$, $p < 0.0001$; subsequent LSM: control naive vs 15 shocks, $p < 0.0001$; control naive vs 30 shocks, $p = 0.0004$; *fur1*^{1} naive vs 15 shocks, $p = 0.0973$; *fur1*^{1} naive vs 30 shocks, $p = 0.0001$).

To ascertain that this was indeed habituation and not fatigue because of the extensive stimulation, the animals were exposed to 8 s of YO, which is known to be an effective dishabituator (Roussou et al., 2019), immediately after the 30th footshock. This resulted in the recovery of shock avoidance to naive levels (Fig. 1*D*; ANOVA: $F_{(5,50)} = 25.4552$, $p < 0.0001$; subsequent LSM: control naive vs 30 shocks, $p < 0.0001$; control 30 shocks vs 30 shocks+YO, $p < 0.0001$; *fur1*^{1} naive vs 30 shocks $p < 0.0001$; *fur1*^{1} 30 shocks vs 30 shocks+YO, $p < 0.0001$), demonstrating that mutants habituate after 30 footshocks, instead of 15 footshocks, which suffice for control animals to habituate. Heterozygotes for the *fur1*^{3} allele, also habituated after 30 footshocks and dishabituated with an 8 s puff of yeast odor (Fig. 1*F*; ANOVA: $F_{(5,41)} = 23.8953$, $p < 0.0001$; subsequent LSM: control naive vs 30 shocks, $p < 0.0001$; control 30 shocks vs 30 shocks + YO, $p < 0.0001$; *fur1*^{3}/+ naive vs 30 shocks, $p < 0.0001$; *fur1*^{3}/+ 30 shocks vs 30 shocks+YO, $p < 0.0001$), indicating that neurons mediating shock habituation are sensitive to Fur1 for timely latency termination and habituation onset by the 15th stimulus, as control animals do (Fig. 1; Acevedo et al., 2007; Roussou et al., 2019). Because 15 footshocks suffice for these and other control strains to habituate (Acevedo et al., 2007; Roussou et al., 2019), we use this stimulus number threshold to compare the performance of mutants and animals with tissue-specific Fur1 attenuation in all subsequent experiments.

However, unlike *dBtk* abrogation (Roussou et al., 2019), the *fur1* mutants did not habituate prematurely to six footshocks (Fig. 1*G*: ANOVA: $F_{(3,55)} = 0.3457$, $p = 0.7924$; and Fig. 1*H*: ANOVA: $F_{(3,50)} = 1.4271$, $p = 0.2467$). Moreover, exposure to the continuous aversive odorant 3-octanol for 4 min, which is known to yield the habituated response (Semelidou et al., 2018), elicited habituation in both controls and *fur1* mutants (Fig. 1*I*: ANOVA:

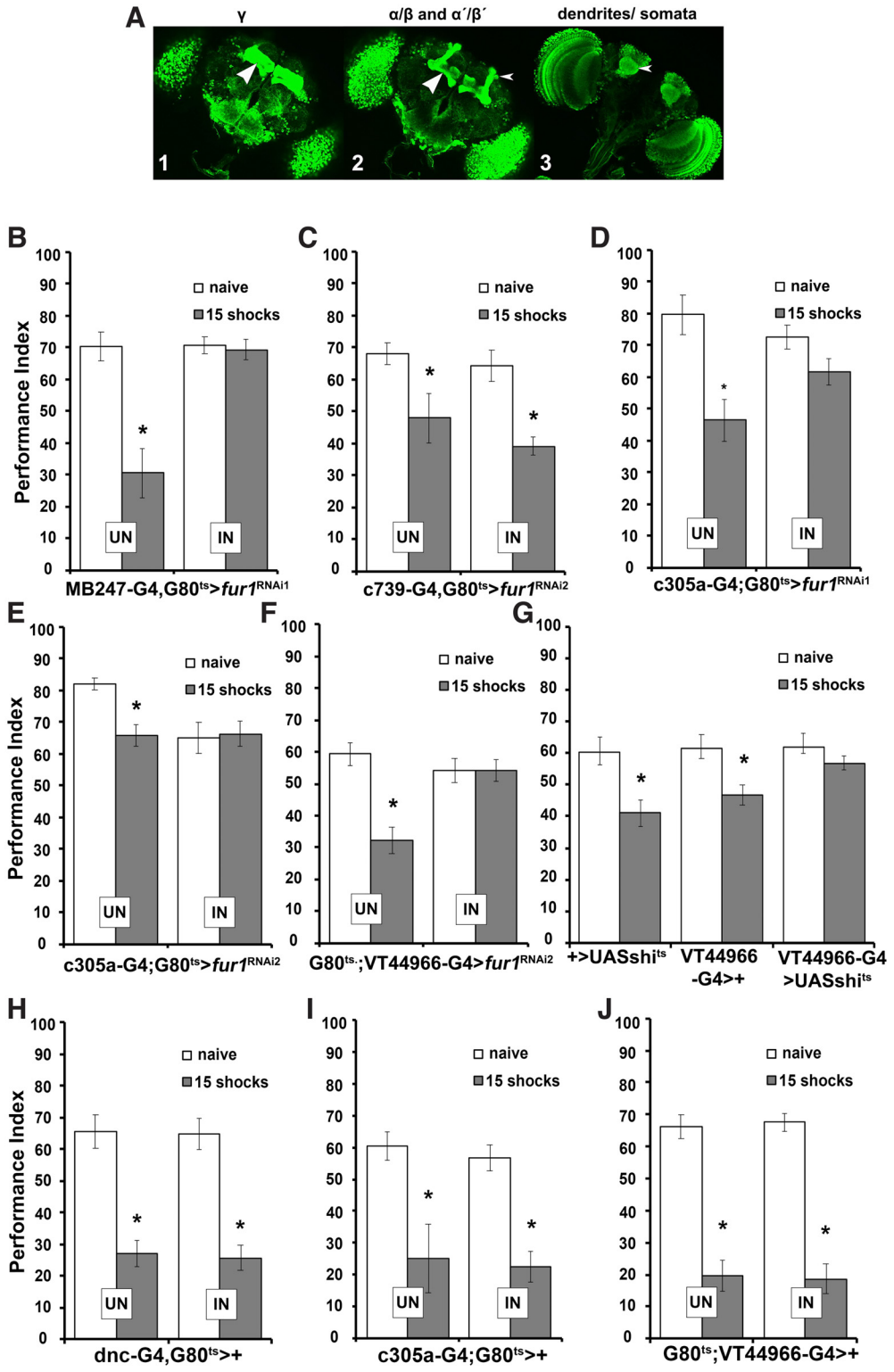

Figure 2. Furin1 is acutely required within MB α'/β' and γ neurons for shock habituation. ***A***, Furin1 is expressed in adult mushroom body neurons, revealed by a gene fragment driving a reporter GFP-expressing transgene as detailed in https://flweb.janelia.org/cgi-bin/view_flew_imagery.cgi?line=R26H09 (Jenett et al., 2012). 1–3, Expression in the γ neurons is highlighted by the large arrowhead (1), in the α/β neurons by a large arrowhead (2) and the α'/β' neurons with a small arrowhead (2), while the respective dendrites and cell bodies by the small arrowhead (3). ***B–J***, Mean ± SEM performance indices calculated as detailed in Materials and Methods are shown. Gray bars represent the response of control and mutant flies to the test foot-shock stimuli after pre-experiencing 15 such shocks. Open bars represent the naïve responses to the test stimuli. Stars indicate significant differences from the naive response, and the collective statistical details are presented in Table 1. ***B***, Avoidance of controls (UN) and flies with RNAi-mediated abrogation of Fur1 within adult MBs under MB247-Gal4, Gal80^{ts} (IN) exposed to 15 foot-shocks or naïve: $n \geq 8$ for all groups. ***C***, Controls (UN) and flies with Fur1 abrogation (IN) in adult α/β MB neurons under c739-Gal4, Gal80^{ts} were assessed for avoidance either naive or exposed to 15 shocks: $n \geq 7$ for all groups. ***D***, Shock avoidance in flies with Fur1 abrogation in adult α'/β' MB neurons under c305a-Gal4; Gal80^{ts} (IN) and controls (UN) exposed to 15 shocks or naïve: $n \geq 10$ for all groups. ***E***, Avoidance of controls (UN) and flies with Fur1 abrogation in adult α'/β' MB neurons under c305-Gal4; Gal80^{ts} (IN) either naive or exposed to 15 shocks: $n = 14$ for all groups. ***F***, Flies with Fur1 abrogation in adult γ MB neurons under Gal80^{ts}; VT44966-Gal4 (IN) and controls (UN) tested for avoidance after pre-exposure to 15 electric shocks or naïve: $n \geq 11$

$F_{(3,54)}$ = 14.0257, $p < 0.0001$; subsequent LSM: control naive vs 4 min OCT, $p = 0.0002$; $fur1^1$ naive vs 4 min OCT, $p < 0.0001$; Fig. 1*J*: ANOVA: $F_{(3,47)}$ = 7.3664, $p = 0.0004$; subsequent LSM: control naive vs 4 min OCT, $p = 0.0036$; $fur1^2$ naive vs 4 min OCT, $p = 0.0010$). This indicates that, in contrast to footshock, Fur1 activity is not required for olfactory habituation. Rather, Fur1 likely operates within specific neuronal circuits of the adult CNS engaged in assessing and mediating responses to footshock stimuli.

Because an antibody to ascertain reduction in Fur1 levels is not available, we sought to confirm that attenuation of this protein indeed results in footshock habituation defects using RNAi. To get insights regarding the spatial restriction of Fur1 RNAi expression, we searched the Janelia library of gene fragments driving reporter expression (Jenett et al., 2012) for the GFP pattern under *fur1* genomic elements. Although broadly expressed (Jenett et al., 2012), Fur1 also appears present within all mushroom body (MB) neuronal subtypes (Fig. 2*A*). The ~2000 neurons in the dorsal posterior per brain hemisphere comprising the MBs project their axons anteriorly forming the horizontal γ, β, and β' lobes, and the vertical α and α' lobes. Given the role of the MBs in the process (Acevedo et al., 2007; Papanikolopoulou et al., 2019; Roussou et al., 2019) and in stimulus modulation (Modi et al., 2020), we used the RNAi-mediating transgenes ($fur1^{RNAi}$) to abrogate Fur1 specifically in postdevelopmental adult MBs using TARGET (McGuire et al., 2004). Consistent with the reporter pattern, RNAi-mediated Fur1 attenuation (IN) in all MB neurons (MBNs) under MB247-Gal4 (Fig. 2*B*) resulted in deficient habituation to 15 footshocks, whereas sibling animals with the RNAi-mediating transgene silent (UN) habituated normally (ANOVA: $F_{(3,34)}$ = 16.3363, $p < 0.0001$; subsequent LSM: UN naive vs UN 15 shocks, $p < 0.0001$; IN naive vs IN 15 shocks, $p = 0.8537$). This independently confirms that the deficit of the *fur1* mutants is indeed because of attenuated Fur1 levels, and it is not developmental in origin.

Processes underlying footshock habituation latency engage the α/β MBNs (Acevedo et al., 2007; Roussou et al., 2019), and, as expected, Fur1 attenuation therein did not result in premature habituation (Fig. 2*C*), as both experimental and control flies responded normally (ANOVA: $F_{(3,29)}$ = 7.911, $p = 0.0007$; subsequent LSM: UN naive vs UN 15 shocks, $p = 0.0092$; IN naive vs IN 15 shocks, $p = 0.0009$). In contrast, animals with attenuated Fur1 within adult α'/β' neurons under c305a-Gal4 (see Fig. 5, expression pattern) whose activation has been reported to be essential for normal habituation (Roussou et al., 2019) did not habituate to 15 shocks in contrast to controls (Fig. 2*D*; ANOVA: $F_{(3,41)}$ = 7.2492, $p = 0.0006$; subsequent LSM: UN naive vs UN 15 shocks, $p = 0.0001$; IN naive vs IN 15 shocks, $p = 0.1398$). This result was independently confirmed with a second RNAi-encoding transgene (Fig. 2*E*; ANOVA: $F_{(3,55)}$ = 5.0754, $p = 0.0037$; subsequent LSM: UN naive vs UN 15 shocks, $p = 0.0027$; IN naive vs IN 15 shocks, $p = 0.7964$).

Interestingly, Fur1 attenuation within γ neurons under VT44966-Gal4 (see Fig. 5, expression pattern) also precipitated defective habituation (Fig. 2*F*; ANOVA: $F_{(3,45)}$ = 10.6144, $p < 0.0001$; subsequent LSM: UN naive vs UN 15 shocks, $p < 0.0001$; IN naive vs IN 15 shocks, $p = 0.9642$). Because to date γ neurons have not been implicated in footshock habituation, we confirmed their role by synaptically silencing them by expression of the temperature-sensitive dynamin shi^{ts} (Kitamoto, 2001). In fact, silencing γ neurons resulted in deficient habituation (Fig. 2*G*; ANOVA: $F_{(5,79)}$ = 5.1596, $p = 0.0004$; subsequent LSM: +>UASshi^{ts} naive vs +>UASshi^{ts} 15 shocks, $p = 0.0009$; VT44966-Gal4>+ naive vs VT44966-Gal4>+ 15 shocks, $p = 0.0063$; VT44966-Gal4>UASshi^{ts} naive vs VT44966-Gal4>UASshi^{ts} 15 shocks, $p = 0.3863$). This result expands the MBNs needed to be synaptically active to drive footshock habituation to include the γ neurons, in addition to α'/β' (Roussou et al., 2019). The RNAi-mediated habituation deficit is not a nonspecific effect of induction by incubation at 30°C for two reasons. First, because although exposed to 30°C for the same amount of time as for animals presenting defects on induction, habituation was normal in animals expressing $fur1^{RNAi2}$ in α/β neurons (Fig. 2*C*). Second, heterozygotes of all drivers that underwent the same induction regime also habituated normally (Fig. 2*H*: ANOVA: $F_{(3,43)}$ = 23.7752, $p < 0.0001$; subsequent LSM: UN naive vs UN 15 shocks, $p < 0.0001$; IN naive vs IN 15 shocks, $p < 0.0001$; Fig. 2*I*: ANOVA: $F_{(3,45)}$ = 11.82, $p < 0.0001$; subsequent LSM: UN naive vs UN 15 shocks, $p = 0.0003$; IN naive vs IN 15 shocks, $p = 0.0001$; Fig. 2*J*: ANOVA: $F_{(3,34)}$ = 43.7431, $p < 0.0001$; subsequent LSM: UN naive vs UN 15 shocks, $p < 0.0001$; IN naive vs IN 15 shocks, $p < 0.0001$). In addition, for $fur1^{RNAi2}$/+ ANOVA: $F_{(3,43)}$ = 9.8354, $p < 0.0001$; subsequent LSM: UN naive vs UN 15 shocks, $p = 0.0013$; IN naive vs IN 15 shocks, $p = 0.0001$. Collectively then, these results verify that the Fur1 attenuation leads to defective footshock habituation. Conversely, Fur1 activity is required within adult α'/β' and γ MBNs for normal footshock habituation.

To validate this conclusion, we aimed to reverse the habituation deficit of $fur1^1$ mutants by the expression of a *fur1* transgene within their α'/β' and γ neurons. Transgenes carrying *Drosophila* or human *fur* cDNAs were introduced to $fur1^1$ mutants and driven in adult $fur1^1$ homozygote MBs under c305a-Gal4 and VT44966-Gal4. Expression of these transgenes in control animals and $fur1^1$ mutant homozygotes under both drivers was verified using PCR (Fig. 3*A*,*E*, UAS*fur1*, *B*,*F*, UAS*hfur*). Although expressed under Gal4, the animals were raised at 18°C to minimize transgene expression during development. In fact, the HA-tagged human protein, which could be assayed with the available anti-HA antibody, was detectable only after a 24 h incubation at 30°C (Fig. 3*I*). Therefore, all experimental animals and relevant controls were incubated at 30°C for 24 h before behavioral experimentation.

Expression of the *Drosophila furin1* transgene (*UASfur1*) in α'/β' neurons (Fig. 3*C*) fully rescued the inability of $fur1^1$ homozygotes to habituate to 15 footshocks (ANOVA: $F_{(7,83)}$ = 5.7847, $p < 0.0001$; subsequent LSM: $fur1^1$ naive vs $fur1^1$ 15 shocks, $p = 0.1819$; c305a-Gal4/+; $fur1^1$/+ naive vs c305a-Gal4/+; $fur1^1$/+ 15 shocks, $p = 0.002$; UAS*fur1*/+; $fur1^1$/+ naive vs UAS*fur1*/+; $fur1^1$/+ 15 shocks, $p < 0.0001$; c305a-G4/UAS*fur1*; $fur1^1$/$fur1^1$ naive vs c305a-G4/UAS*fur1*; $fur1^1$/$fur1^1$ 15 shocks, $p = 0.0062$). Importantly, expression of the human *Furin* cDNA within $fur1^1$ homozygote α'/β' neurons also fully rescued their deficient habituation (Fig. 3*D*; ANOVA: $F_{(7,64)}$ = 19.4922, $p < 0.0001$; subsequent LSM: $fur1^1$ naive vs $fur1^1$ 15 shocks, $p = 0.6838$; c305a-Gal4/+; $fur1^1$/+ naive vs c305a-Gal4/+; $fur1^1$/+ 15 shocks, $p < 0.0001$; UAS*hfur*, $fur1^1$/+ naive vs

←

for all groups. ***G***, Avoidance of controls (+>UAS-shi^{ts} and VT44966-Gal4>+) and flies with silenced adult γ MB neurons after exposure to 15 electric shocks, or naive: $n \geq 11$ for all groups. ***H–J***, UN and IN heterozygotes of the indicated Gal4 driver lines were assessed for avoidance after pre-exposure to 15 shocks or naive. Both UN and IN were raised at 18°C until hatching, and then IN were incubated at 30°C for 48 h to emulate induction while UN remained at 18°C: $n \geq 8$ for all groups.

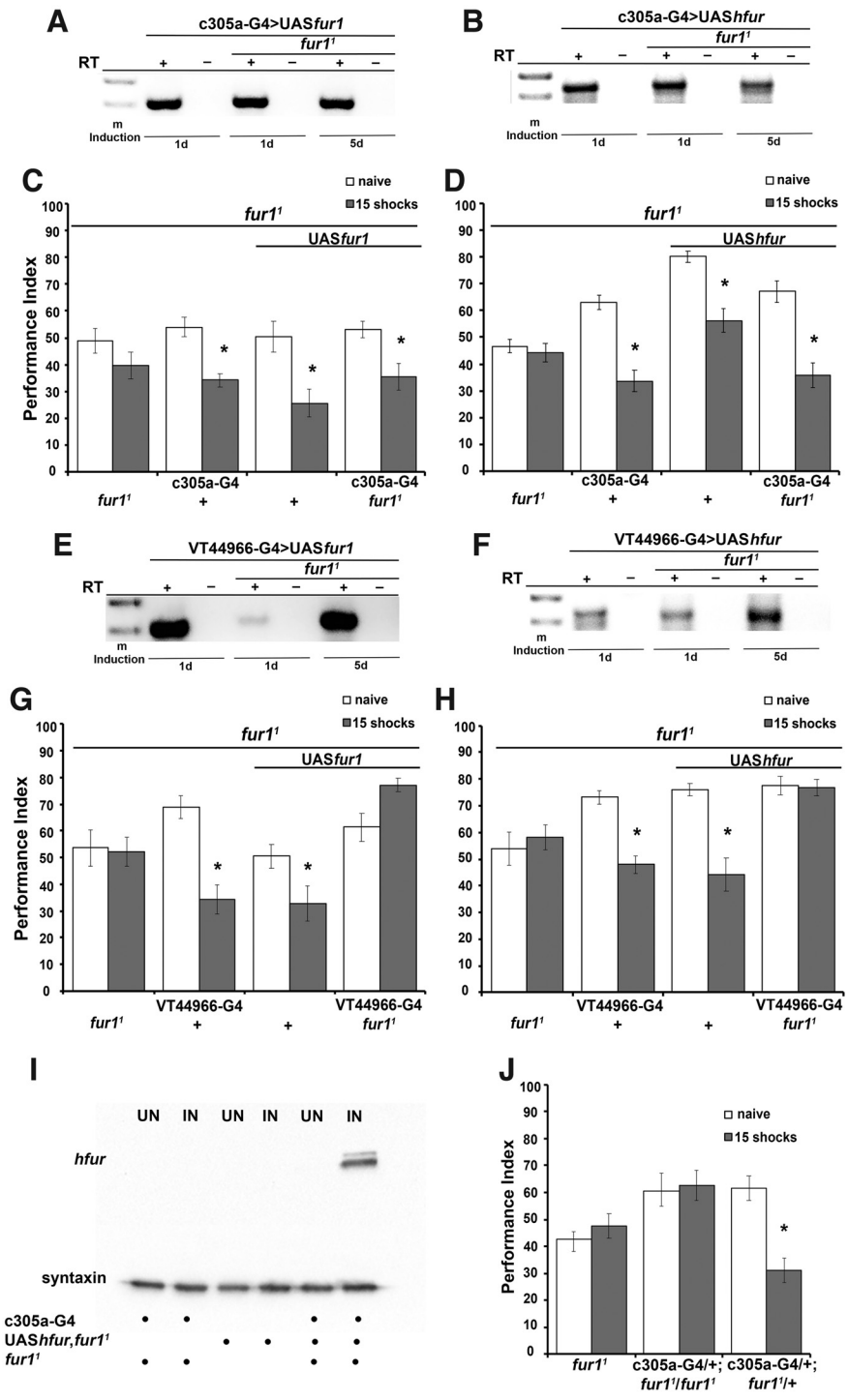

Figure 3. Genetic rescue of the footshock habituation deficit with *Drosophila* and human Furin transgenes. ***C***, ***D***, ***G***, ***H***, ***J***, Mean ± SEM performance indices calculated as detailed in Materials and Methods are shown. Gray bars represent the response of control and mutant flies to the test footshock stimuli after pre-experiencing 15 such shocks. Open bars represent the naive responses to the test stimuli. All experimental animals were raised at 18°C and shifted to 30°C for 24 h to drive the expression of Furin transgenes. Control heterozygotes were treated similarly. The "+" on the graphs (***C***, ***D*** and ***G***, ***H***) is used to discriminate $fur1^1$ heterozygotes from the $fur1^1$ homozygotes. Stars indicate significant differences from the naive response, and the collective statistical details are presented in Table 1. ***A***, ***B***, ***E***, ***F***, Results of PCR after reverse transcription (RT+) or without (RT–) of transgene-encoded RNAs expressed in $fur1^1$ homozygotes or in wild-type animals (first two lanes) under the α'/β' driver c305a-Gal4 (***A***, ***B***), or the γ driver VT44966-Gal4 (***E***, ***F***). Transgene-specific transcripts were selected and reverse transcribed with specific reverse primers, while amplification of transgene-specific cDNAs was achieved with specific forward primers and the reverse primers used for reverse transcription. The *Drosophila* transgene is assayed for expression in ***A*** and ***E***, and the human transgene in ***B*** and ***F***. Experimental animals were raised at 18°C and 2- to 3-d-old adults were shifted to 30°C for 24 h (1 d) or 120 h (5 d) to induce the transgenes. *m* denotes the size marker between 200 and 300 bp. Since the sought results are qualitative (i.e., expression or not), there are no loading or efficiency controls. ***C***, UAS*hfur*, $fur1^1$/+ 15 shocks, $p < 0.0001$; c305a-G4/+; UAS*hfur*, $fur1^1/fur1^1$ naive vs c305a-G4/+; UAS*hfur*, $fur1^1/fur1^1$ 15 shocks, $p < 0.0001$). This indicates that the human protein is functionally orthologous with Fur1. In fact, comparison of the *Drosophila* with the human sequence using DIOPT version 8.0 (https://www.flyrnai.org/cgi-bin/DRSC_prot_align.pl?geneid1=47220&geneid2=5045) demonstrates that both are members of the protein convertase family, with overall 53% identity and 65% similarity. The identities are primarily distributed over recognizable functional domains, namely 53% over the N terminus proximal S8 serine-type endopeptidase family domain, 71% over the Kexin-like domain, and 73% over the central S8 peptidase family domain.

Based on the above, the consequences of Fur1 loss within MBNs could be reflective of Furin attenuation in the human CNS, which has been linked to schizophrenia (Fromer et al., 2016, Christensen and Børglum, 2019; Schrode et al., 2019). Hence, as Fur1 loss is complemented by its conserved human homolog, the collective results suggest that footshock habituation defects constitute a potential schizophrenia protophenotype in *Drosophila*. Reversal of the habituation deficit depended on transgene expression as the driver alone did not rescue the defect (Fig. 3*J*; ANOVA: $F_{(5,55)} = 6.8503$, $p < 0.0001$; subsequent LSM: $fur1^1$ naive vs $fur1^1$ 15 shocks, $p = 0.5362$; c305a-G4/+; $fur1^1/fur1^1$ naive vs c305a-G4/+; $fur1^1/fur1^1$ 15 shocks, $p = 0.7692$; c305a-G4/+; $fur1^1$/+ naive vs c305a-G4/+; $fur1^1$/+ 15 shocks, $p < 0.0001$). Therefore,

←

Avoidance of controls and flies expressing a *Drosophila furin1* transgene (*UASfur1*) in adult $fur1^1$ α'/β' MB neurons exposed to 15 shocks or naïve: $n \geq 8$ for all groups. ***D***, Shock avoidance in controls and flies expressing a human *furin* transgene (*UAShfur*) in adult $fur1^1$ α'/β' MB neurons exposed to 15 shocks or naïve: $n \geq 7$ for all groups. ***G***, Controls and flies expressing a *Drosophila furin1* transgene (*UASfur1*) in adult $fur1^1$ γ MB neurons were assessed for avoidance after pre-exposure to 15 electric footshocks or naïve: $n \geq 9$ for all groups. ***H***, Investigation of avoidance in flies with the expression of a human *furin* transgene (*UAShfur*) in adult $fur1^1$ γ MB neurons and controls exposed to 15 shocks or naïve: $n \geq 6$ for all groups. ***I***, Assessment of *hfur* expression using the anti-HA-Tag antibody in c305a-G4/+; UAS*hfur*, $fur1^1/fur1^1$ flies. The experimental animals were raised at 18°C (UN) and 2- to 3-d-old adults were shifted to 30°C for 24 h (IN) to drive expression of the human Furin transgene. Control heterozygotes were treated similarly. ***J***, Avoidance in $fur1^1$ mutant homozygotes and heterozygotes carrying the c305a-G4 driver (c305a-G4/+; $fur1^1/fur1^1$) exposed to 15 shocks or naïve: $n \geq 8$ for all groups.

Fur1 expression in α'/β' neurons appears necessary and sufficient to support mechanisms requisite for normal habituation to footshocks.

In contrast, the expression of either *Drosophila* (Fig. 3*G*) or human transgenes (Fig. 3*H*) within the γ neurons did not reverse the habituation deficit of *fur1*^{1} homozygotes (Fig. 3*G*: ANOVA: $F_{(7,75)} = 8.0094$, $p < 0.0001$; subsequent LSM: *fur1*^{1} naive vs *fur1*^{1} 15 shocks, $p = 0.8525$; VT44966-G4, *fur1*^{1}/+ naive vs VT44966-G4, *fur1*^{1}/+ 15 shocks, $p < 0.0001$; UAS*fur1*/+; *fur1*^{1}/+ naive vs UAS*fur1*/+; *fur1*^{1}/+ 15 shocks, $p < 0.0006$; UAS*fur1*/+; VT44966-G4, *fur1*^{1}/*fur1*^{1} naive vs UAS*fur1*/+; VT44966-G4, *fur1*^{1}/*fur1*^{1} 15 shocks, $p < 0.04471$; Fig. 3*H*: ANOVA: $F_{(7,55)} = 9.3652$, $p < 0.0001$; subsequent LSM: *fur1*^{1} naive vs *fur1*^{1} 15 shocks, $p = 0.4541$; VT44966-G4, *fur1*^{1}/+ naive vs VT44966-G4, *fur1*^{1}/+ 15 shocks, $p = 0.0004$; UAS*hfur*, *fur1*^{1}/+ naive vs UAS*hfur*, *fur1*^{1}/+ 15 shocks, $p < 0.0001$; VT44966-G4, *fur1*^{1}/UAS*hfur*, *fur1*^{1} naive vs VT44966-G4, *fur1*^{1}/UAS*hfur*, *fur1*^{1} 15 shocks, $p = 0.9124$). Lack of rescue under the γ driver was apparent even after prolonged transgene expression for 2 and 5 d at 30°C, respectively (Table 2). Because Fur1 abrogation therein resulted in habituation deficits (Fig. 2*F*) and neurotransmission from γ neurons is required for footshock habituation (Fig. 2*G*), Fur1 activity within these neurons is necessary for the process. However, lack of rescue when α'/β' neurons are mutant indicates that Fur1 is not cell autonomously sufficient within γ neurons to drive habituation.

It should also be noted that although the habituation assay yields somewhat variable results, the performance of mutants and animals with abrogated Fur1 is consistently defective over multiple independent experiments in different genetic backgrounds, as detailed above and below and summarized in the statistics table (Table 1).

Table 2. Extended transgene expression in γ neurons fails to rescue the habituation deficit of *fur1*^{1} mutant homozygotes

Genotype	Mean ± SEM	*F* ratio	*p*
UAS*fur1*/+; VT44966-G4, *fur1*^{1}/ *fur1*^{1}			
2 d induction			
ANOVA $F_{(7,103)} = 6.1248$, $p < 0.0001$			
fur1^{1} (naive)	56.47 ± 4.49	0.1429	0.7062
fur1^{1} (15 shocks)	53.80 ± 3.70		
VT44966-G4, *fur1*^{1}/+ (naive)	57.40 ± 5.55	22.0973	<0.0001
VT44966-G4, *fur1*^{1}/+ (15 shocks)	28.04 ± 5.57		
UAS*fur1*/+; *fur1*^{1}/+ (naive)	58.46 ± 3.82	9.8189	0.0023
UAS*fur1*/+; *fur1*^{1}/+ (15 shocks)	39.22 ± 2.60		
UAS*fur1*/+; VT44966-G4, *fur1*^{1}/ *fur1*^{1} (naive)	58.33 ± 4.92	2.0107	0.1594
UAS*fur1*/+; VT44966-G4, *fur1*^{1}/ *fur1*^{1} (15 shocks)	48.95 ± 5.04		
VT44966-G4, *fur1*^{1}/UAS*hfur*, *fur1*^{1}			
2 d induction			
ANOVA $F_{(7,84)} = 11.2156$, $p < 0.0001$			
fur1^{1} (naive)	50.30 ± 3.98	0.0094	0.9232
fur1^{1} (15 shocks)	49.61 ± 5.20		
VT44966-G4, *fur1*^{1}/+ (naive)	72.98 ± 4.39	42.1933	<0.0001
VT44966-G4, *fur1*^{1}/+ (15 shocks)	28.98 ± 7.10		
UAS*hfur*, *fur1*^{1}/+ (naive)	63.02 ± 4.68	26.1768	<0.0001
UAS*hfur*, *fur1*^{1}/+ (15 shocks)	29.84 ± 3.76		
VT44966-G4, *fur1*^{1}/UAS*hfur*, *fur1*^{1} (naive)	64.97 ± 4.46	1.3436	0.25
VT44966-G4, *fur1*^{1}/UAS*hfur*, *fur1*^{1} (15 shocks)	56.51 ± 4.33		
UAS*fur1*/+; VT44966-G4, *fur1*^{1}/ *fur1*^{1}			
5 d induction			
ANOVA $F_{(7,72)} = 10.9129$, $p < 0.0001$			
fur1^{1} (naive)	63.29 ± 4.28	0.3224	0.5721
fur1^{1} (15 shocks)	60.02 ± 2.65		
VT44966-G4, *fur1*^{1}/+ (naive)	59.45 ± 5.96	13.5777	0.0005
VT44966-G4, *fur1*^{1}/+ (15 shocks)	36.97 ± 4.56		
UAS*fur1*/+; *fur1*^{1}/+ (naive)	64.33 ± 3.49	38.0843	<0.0001
UAS*fur1*/+; *fur1*^{1}/+ (15 shocks)	25.35 ± 4.95		
UAS*fur1*/+; VT44966-G4, *fur1*^{1}/ *fur1*^{1} (naive)	60.37 ± 3.31	0.1046	0.7474
UAS*fur1*/+; VT44966-G4, *fur1*^{1}/ *fur1*^{1} (15 shocks)	61.98 ± 3.41		
VT44966-G4, *fur1*^{1}/UAS*hfur*, *fur1*^{1}			
5 d induction			
ANOVA $F_{(7,70)} = 7.8879$, $p < 0.0001$			
fur1^{1} (naive)	55.61 ± 4.29	0.3895	0.5348
fur1^{1} (15 shocks)	59.83 ± 4.29		
VT44966-G4, *fur1*^{1}/+ (naive)	68.36 ± 3.98	30.4706	<0.0001
VT44966-G4, *fur1*^{1}/+ (15 shocks)	29.00 ± 5.64		
UAS*hfur*, *fur1*^{1}/+ (naive)	58.48 ± 6.01	10.829	0.0016
UAS*hfur*, *fur1*^{1}/+ (15 shocks)	34.29 ± 7.03		
VT44966-G4, *fur1*^{1}/UAS*hfur*, *fur1*^{1} (naive)	63.50 ± 4.56	0.0889	0.7666
VT44966-G4, *fur1*^{1}/UAS*hfur*, *fur1*^{1} (15 shocks)	61.24 ± 4.02		

Avoidance assessment of flies expressing a *Drosophila furin1* transgene (*UASfur1*) or a human *furin* transgene (*UAShfur*) in adult *fur1*^{1} γ MB neurons for 2 or 5 d and in control heterozygotes exposed to 15 electric shocks or naive. All experimental animals were raised at 18°C, and 2- to 3-d-old adults were kept at 30°C for the indicated 2 or 5 d to induce (IN) the Fur1 transgenes. Control heterozygotes were treated similarly.

Pharmacological amelioration of habituation deficits on Fur1 abrogation

Polymorphisms that ostensibly lead to Furin attenuation have been linked to schizophrenia in humans (Sharma et al., 2009; Fromer et al., 2016, Schrode et al., 2019), with antipsychotics being the main treatment course. Thus, antipsychotics were used to attempt reversal of the habituation defects on Fur1 loss as these drugs have been reported to be effective in reversing footshock habituation defects (Roussou et al., 2019). There are two main classes of antipsychotics, typical and atypical, thought to address with broadly variable affinities a number of receptors. These include primarily serotonin and dopamine receptors, but also muscarinic, adrenergic, glutamatergic, and histaminic receptors (Kapur and Mamo, 2003; van Os and Kapur, 2009; Patel et al., 2014). Typical antipsychotics, such as haloperidol appear to antagonize mainly the DRD2 dopamine receptor (Kapur and Mamo, 2003), while the atypical clozapine and risperidone are thought to be potent antagonists of catecholamine receptors, with the HTR2A being a primary target (Patel et al., 2014).

Since Fur1 activity is required for habituation in specific MBNs (Figs. 2, 3), we opted to treat pharmacologically animals where the protein was specifically abrogated therein. We used drug concentrations in the low-nanomolar range to avoid nonspecific effects because of drug excess. Because we offer the drugs orally with unknown, at the moment, pharmacodynamics and pharmacokinetics, it is reasonable that the concentration reaching the fly CNS and the neurons lacking Fur1, must be significantly lower than that added in the food and reported below.

The deficient habituation on conditional Fur1 abrogation within α'/β' neurons was reversed by the typical antipsychotic haloperidol specifically at 10 nM, but not at lower (Fig. 4*A*; ANOVA: $F_{(9,111)} = 3.3112$, $p = 0.0014$; subsequent LSM: UN vehicle naive vs UN vehicle 15 shocks, $p = 0.0013$; IN vehicle naive vs IN vehicle 15 shocks, $p = 0.5039$; IN 2 nM haloperidol naive vs IN 2 nM haloperidol 15 shocks, $p = 0.1774$; IN 5 nM haloperidol naive vs IN 5 nM haloperidol 15 shocks, $p = 0.2412$; IN 10 nM haloperidol naive vs IN 10 nM haloperidol 15 shocks, $p = 0.0087$).

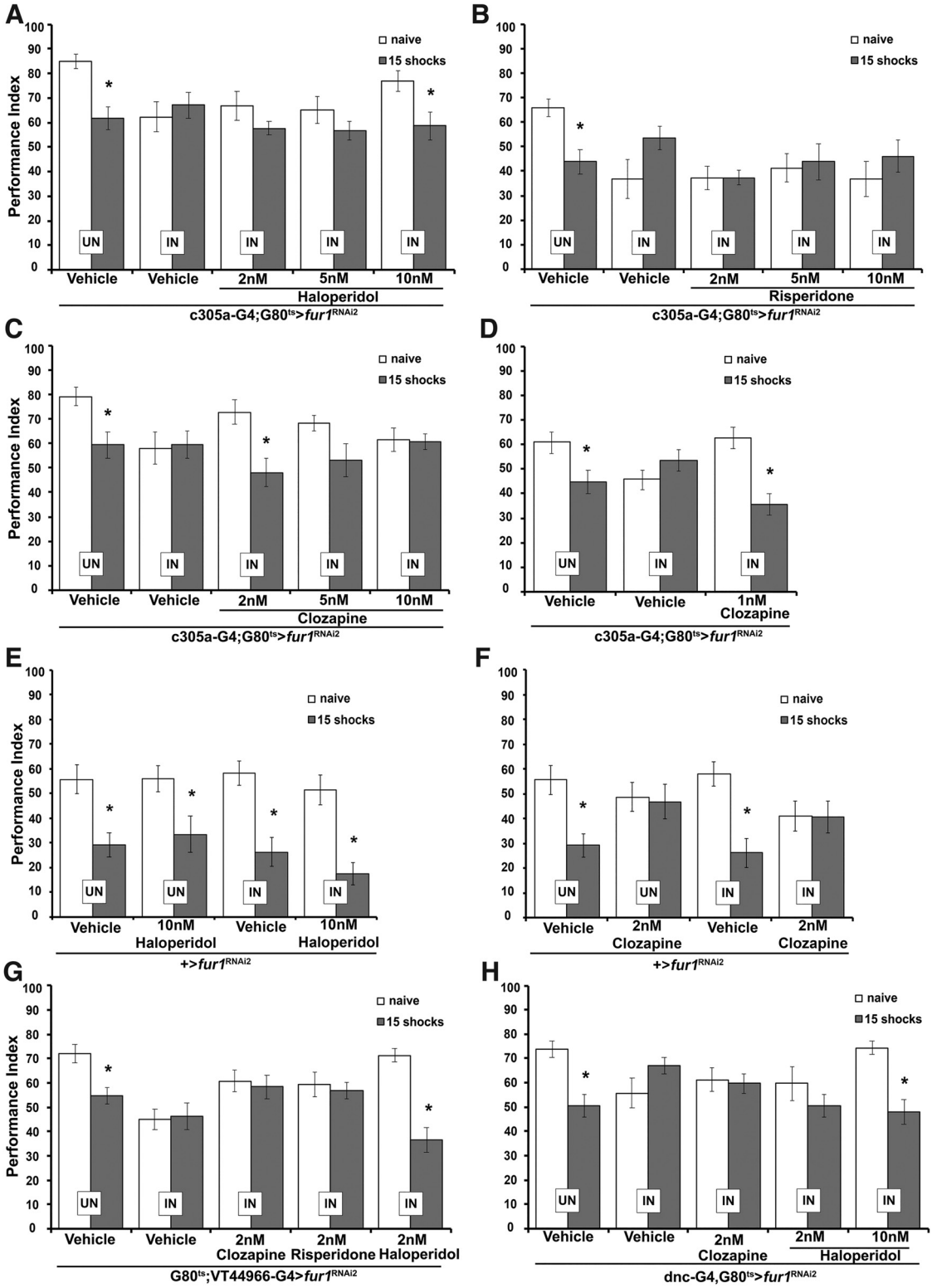

Figure 4. Selective pharmacological reversal of deficient footshock habituation on Fur1 attenuation in MB neurons. Mean ± SEM performance indices calculated as detailed in Materials and Methods are shown. Gray bars represent the response of control and mutant flies to the test footshock stimuli after pre-experiencing 15 such shocks. Open bars represent the naive responses to the test stimuli. All pharmaceuticals were dissolved in DMSO (vehicle) and delivered in yeast paste as a sole food source for 14–16 h. Stars indicate significant differences from the naive response, and the collective statistical details are presented in Table 1. ***A***, Shock avoidance in flies with adult-specific Fur1 abrogation (IN) in α'/β'MB neurons treated with haloperidol as indicated and vehicle-treated control animals either exposed to 15 shocks or naïve: $n \geq 11$ for all groups. ***B***, Similarly, avoidance of animals exposed to 15 shocks and naive animals with adult-specific Fur1 abrogation (IN) in adult α'/β'MB neurons treated with risperidone as indicated and of vehicle-treated controls was assessed. $n \geq 11$ for all groups. ***C***, Animals with Fur1 abrogation (IN) within adult α'/β'MB neurons were assessed for avoidance after treatment with clozapine as indicated and vehicle-treated controls, after exposure to 15 footshocks or naïve: $n \geq 9$ for all groups. ***D***, Shock avoidance of animals with Fur1 abrogation (IN) in adult α'/β'MB neurons treated with vehicle or 1 nM clozapine and of vehicle-treated controls exposed to 15 shocks or naive: $n \geq 8$ for all groups. ***E***, Vehicle-treated or haloperidol-treated $+>fur1^{RNAi2}$ kept at 18°C (UN) or shifted to 30°C for 48 h (IN) were tested for shock avoidance after exposure to 15 footshocks and naive: $n = 11$ for all groups. ***F***, Similarly, Vehicle-treated or clozapine-treated $+>fur1^{RNAi2}$ kept at 18°C (UN) or shifted to 30°C for 48 h (IN) were tested for avoidance

To test whether Fur1 loss in α'/β' MBNs is ameliorated specifically by haloperidol, we used the also commonly used atypical antipsychotic risperidone, which had rescued the footshock habituation deficit of *Drosophila dBtk* mutants (Roussou et al., 2019). However, risperidone did not reverse the habituation deficit at any of the tested concentrations (Fig. 4*B*; ANOVA: $F_{(9,113)} = 2.6165$, $p = 0.0091$; subsequent LSM: UN vehicle naive vs UN vehicle 15 shocks, $p = 0.006$; IN vehicle naive vs IN vehicle 15 shocks, $p = 0.045$; IN 2 nM risperidone naive vs IN 2 nM risperidone 15 shocks, $p = 0.9909$; IN 5 nM risperidone naive vs IN 5 nM risperidone 15 shocks, $p = 0.7684$; IN 10 nM risperidone naive vs IN 10 nM risperidone 15 shocks, $p = 0.2676$). Because risperidone rescues the deficient habituation of *dBtk* mutants (Roussou et al., 2019), lack of rescue herein is unlikely because of the limited efficacy of the drug and suggests that Fur1 attenuation may affect receptors whose activity is not affected by risperidone.

However, the also atypical antipsychotic clozapine known to antagonize serotonin (5-HT2A mostly) and secondarily dopamine receptors (Naheed and Green, 2001), reversed the habituation deficit on Fur1 loss in α'/β' neurons at 2 nM (Fig. 4*C*; ANOVA: $F_{(9,110)} = 2.9796$, $p = 0.0035$; subsequent LSM: UN vehicle naive vs UN vehicle 15 shocks, $p = 0.0017$; IN vehicle naive vs IN vehicle 15 shocks, $p = 0.8222$; IN 2 nM clozapine naive vs IN 2 nM clozapine 15 shocks, $p = 0.0032$; IN 5 nM clozapine naive vs IN 5 nM clozapine 15 shocks, $p = 0.3993$; IN 10 nM clozapine naive vs IN 10 nM clozapine 15 shocks, $p = 0.9038$), or 1 nM (Fig. 4*D*; ANOVA: $F_{(5,60)} = 5.979$, $p = 0.0002$; subsequent LSM: UN vehicle naive vs UN vehicle 15 shocks, $p = 0.0097$; IN vehicle naive vs IN vehicle 15 shocks, $p = 0.2329$; IN 1 nM clozapine naive vs IN 1 nM clozapine 15 shocks, $p < 0.0001$).

Significantly, a higher concentration of these antipsychotics did not reverse the deficit (Table 3), strongly suggesting that lack of rescue, especially in the case of risperidone, is not because low levels of the drug reach the affected α'/β'neurons. In fact, at higher concentrations the drugs may inhibit or activate additional receptors, with the collective result being lack of rescue. This is apparent with clozapine where the lower concentrations rescue the phenotype, but higher concentrations do not (Fig. 4*C*, *D*). This notion was tested further by exposing control animals (*fur1*^{RNAi2} heterozygotes) to the rescuing concentrations of haloperidol, which did not affect footshock habituation (Fig. 4*E*; ANOVA: $F_{(7,87)} = 8.124$, $p < 0.0001$; subsequent LSM: UN vehicle naive vs UN vehicle 15 shocks, $p = 0.0014$; UN 10 nM haloperidol naive vs UN 10 nM haloperidol 15 shocks, $p = 0.0058$; IN vehicle naive vs IN vehicle 15 shocks, $p = 0.0001$; IN 10 nM haloperidol naive vs IN 10 nM haloperidol 15 shocks, $p < 0.0001$) and clozapine, which resulted in defective footshock habituation (Fig. 4*F*; ANOVA: $F_{(7,87)} = 3.7428$, $p = 0.0015$; subsequent LSM: UN vehicle naive vs UN vehicle 15 shocks, $p = 0.0022$; UN 2 nM clozapine naive vs 2 nM clozapine 15 shocks, $p = 0.8286$; IN vehicle naive vs IN vehicle 15 shocks, $p = 0.0003$; IN 2 nM clozapine naive vs IN 2 nM clozapine 15 shocks, $p = 0.9767$). These results argue that in control flies clozapine, even at the 2 nM concentration, affects receptors implicated in normal footshock habituation. It is unclear at the moment whether on Fur1 attenuation clozapine affects the same receptors to mediate normal habituation. It is rather more likely that the drug acts on multiple target receptors in many neurons, which in the case of control animals shifts the balance toward inhibition of habituation and restores that balance in animals with depleted Furin specifically in their α'/β' MBNs.

Table 3. A Higher dose of antipsychotics does not rescue the habituation deficit of animals with abrogated *fur1*^{1} in their α'/β' mushroom body neurons

Genotype	Mean ± SEM	*F* ratio	*p*
c305a-G4;G80^{ts}>*fur1*^{RNAi2}			
ANOVA $F_{(9,156)} = 2.6871$, $p = 0.0064$			
UN vehicle (naive)	73.27 ± 3.12	12.9585	0.0004
UN vehicle (15 shocks)	52.26 ± 4.03		
IN vehicle (naive)	55.76 ± 3.84	0.6796	0.411
IN vehicle (15 shocks)	60.78 ± 2.52		
IN 10 μM haloperidol (naive)	63.18 ± 5.0	0.0098	0.9211
IN 10 μM haloperidol (15 shocks)	63.77 ± 3.38		
IN 10 μM risperidone (naive)	49.91 ± 5.40	2.3211	0.1298
IN 10 μM risperidone (15 shocks)	58.89 ± 4.32		
IN 10 μM clozapine (naive)	56.98 ± 5.25	0.0575	0.8108
IN 10 μM clozapine (15 shocks)	55.54 ± 4.31		

Animals with abrogated Fur1 in α'/β' neurons and relevant nonexpressing controls, treated as indicated, were assessed for shock avoidance after pre-exposure to 15 shocks or naive. All pharmaceuticals were dissolved in DMSO (vehicle) and delivered in yeast paste as a sole food source for 14–16 h.

Because Fur1 in γ neurons is necessary, but not sufficient to facilitate habituation to footshocks, we addressed the possibility that these neurons will respond differently to pharmaceutical amelioration. Interestingly, animals with attenuated Fur1 in γ neurons habituated normally when treated with 2 nM haloperidol, but not with 2 nM clozapine or 2 nM risperidone (Fig. 4*G*; ANOVA: $F_{(9,86)} = 6.7678$, $p < 0.0001$; subsequent LSM: UN vehicle naive vs UN vehicle 15 shocks, $p = 0.0026$; IN vehicle naive vs IN vehicle 15 shocks, $p = 0.8456$; IN 2 nM risperidone naive vs IN 2 nM risperidone 15 shocks, $p = 0.6899$; IN 2 nM haloperidol naive vs IN 2 nM haloperidol 15 shocks, $p < 0.0001$). This response profile is distinct from that of α'/β' Fur1-depleted neurons, which respond to 10 nM, but not 2 nM haloperidol (Fig. 4*A*) and 2 nM clozapine (Fig. 4*C*). This difference may reflect differential distribution of targeted receptors in these two neuronal populations (Aso et al., 2019), with perhaps more receptor types affected by Fur1 loss in α'/β' than in γ neurons.

To address this hypothesis, we abrogated Fur1 throughout adult MB neurons using the dnc-Gal4 driver (Fig. 5, expression pattern). These flies were treated with clozapine and haloperidol at the concentrations that reversed the habituation defect when the protein was attenuated either in α'/β' or γ neurons. Importantly, the robust habituation deficit on Fur1 loss throughout the MBs (Fig. 4*H*), was fully rescued only with 10 nM, but not 2 nM, haloperidol or 2 nM clozapine (Fig. 4*H*; ANOVA: $F_{(9,143)} = 3.8072$, $p = 0.0003$; subsequent LSM: UN vehicle naive vs UN vehicle 15 shocks, $p = 0.0005$; IN vehicle naive vs IN vehicle 15 shocks, $p = 0.1157$; IN 2 nM clozapine naive vs IN 2 nM clozapine 15 shocks, $p = 0.8114$; IN 2 nM haloperidol naive vs IN 2 nM haloperidol 15 shocks, $p = 0.174$; IN 10 nM haloperidol naive vs IN 10 nM haloperidol 15 shocks, $p = 0.0002$). This indicates that pharmacological reversal of the consequences of Fur1 loss in α'/β' neurons with 10 nM haloperidol suffices to drive normal habituation, confirming the necessary and sufficient role of these neurons in the process. Clozapine appears to be effective only when Fur1 is abrogated in α'/β', but not in γ neurons, suggesting that haloperidol addresses receptors in both types of neurons.

←

after exposure to 15 shocks and naïve: $n = 11$ for all groups. ***G***, Avoidance of exposed and naive animals with Fur1 abrogation in adult γ MB neurons treated as indicated and vehicle-treated controls: $n \geq 8$ for all groups. ***H***, Animals with targeted abrogation of Fur1 throughout adult MBs were pharmacologically treated as indicated and assessed along with vehicle-treated controls for shock avoidance after pre-exposure to 15 shocks or naïve: $n \geq 13$ for all groups.

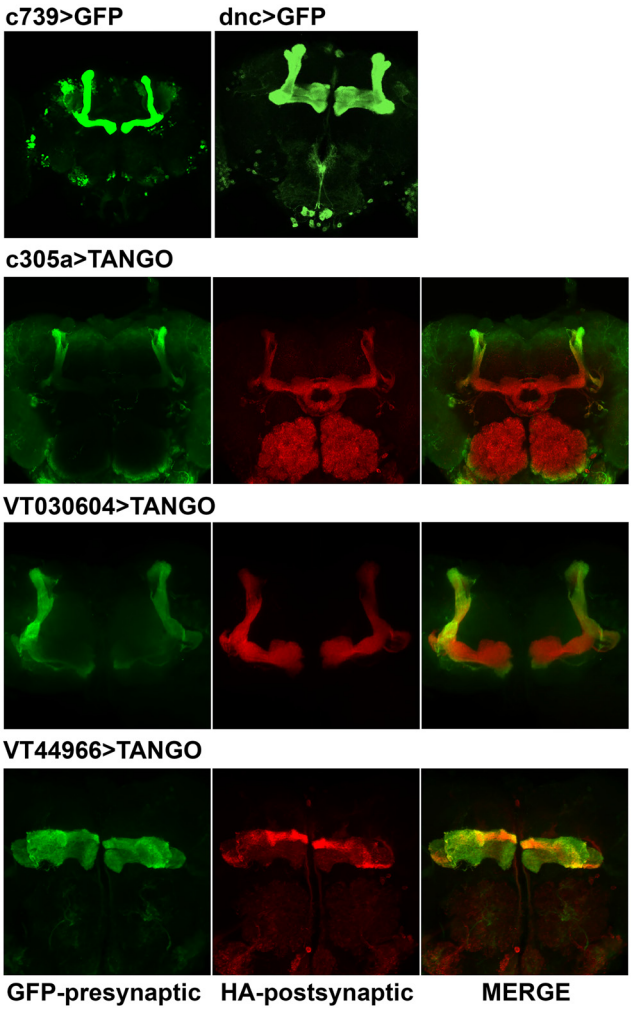

Figure 5. Presynaptic and postsynaptic connections of α'/β' and γ mushroom body neurons. The expression patterns of the c739-Gal4 and dnc-Gal4 revealed by the reporter GFP-expressing transgene (top row). Bottom three rows, Presynaptic neurons are marked with the GFP pattern (green) also detailing the expression patterns of c305a-Gal4 and VT030604-Gal4 for α'/β' neurons and VT44966-Gal4 for γ neurons. The postsynaptic pattern of these neurons is revealed by the anti-HA pattern (red), while the merged panels denote the overlap of the two patterns, which is not obvious.

Table 4. The sex of the experimental animals does not affect drug responsiveness

Genotype	Treatment	Gender	Mean ± SEM	*F* ratio	*p*
w^{1118} x $fur1^{RNAi2}$ ANOVA $F_{(23,263)} = 3.2155$, $p < 0.0001$					
UN (naive)	Vehicle	Females	51.62 ± 7.45	0.4664	0.4953
		Males	58.51 ± 4.81		
UN (15 shocks)	Vehicle	Females	32 ± 7.5	0.6585	0.4179
		Males	23.82 ± 7.45		
UN (naive)	2 nM clozapine	Females	48.35 ± 7.64	0.005	0.9439
		Males	49.06 ± 6.98		
UN (15 shocks)	2 nM clozapine	Females	44.2 ± 7.41	0.2012	0.6542
		Males	48.72 ± 7.67		
UN (naive)	10 nM haloperidol	Females	58.43 ± 6.28	0.4297	0.5128
		Males	51.82 ± 7.2		
UN (15 shocks)	10 nM haloperidol	Females	32.86 ± 7.94	0.0338	0.8543
		Males	34.72 ± 8.93		
IN (naive)	Vehicle	Females	62.93 ± 7.26	0.7768	0.379
		Males	54.04 ± 7.33		
IN (15 shocks)	Vehicle	Females	32.21 ± 5.85	0.0629	0.8022
		Males	29.68 ± 7.26		
IN (naive)	2 nM clozapine	Females	39.08 ± 8.63	0.0688	0.7933
		Males	41.72 ± 6.29		
IN (15)	2 nM clozapine	Females	42.11 ± 7.75	0.086	0.7696
		Males	39.15 ± 6.79		
IN (naive)	10 nM haloperidol	Females	50.08 ± 6.32	0.041	0.8396
		Males	52.13 ± 7.36		
IN (15 shocks)	10 nM haloperidol	Females	21.30 ± 5.59	0.7823	0.3773
		Males	12.38 ± 5.96		

To determine whether the sex of the animals impacted their behavioral output, possibly because of differential yeast paste consumption by the females, mixed-sex +>$fur1^{RNAi2}$ ($fur1^{RNAi2}$ flies crossed with the w^{1118} genetic background of all drivers used) populations were treated with vehicle or antipsychotics at the relevant concentrations after standard 2 d induction at 30°C or uninduced at 18°C, trained as mixed populations, but the PIs of males and females were calculated separately.

Because antipsychotics are offered mixed in yeast paste, we wanted to ascertain that because of their larger size and reproduction-dependent metabolic demands females do not ingest more. Differences in drug ingestion might result in sex-specific differential rescue, increasing the variability of each experimental repetition and skewing results depending on the male/female proportion of the mixed sex populations used in these experiments. To address this issue, we fed vehicle, clozapine, and haloperidol at the rescuing concentrations to mixed sex populations of control flies ($fur1^{RNAi2}$ heterozygotes) kept at 18°C (UN), where metabolism is thought to be relatively lower relative to flies kept under transgene induction conditions at 30°C (IN). These mixed sex populations were subjected to habituation protocols, but their responses were scored separately for males and females within each group. As demonstrated in Table 4, sex-specific statistical differences were not uncovered regardless of treatment or incubation temperature, indicating that differential sex-specific drug consumption does not affect the results.

Collectively, these results demonstrate that antipsychotics are efficacious and relatively specific in reversing habituation deficits of *Drosophila* mutants in a gene linked to schizophrenia in humans. Interestingly, the selective rescue with the typical antipsychotic haloperidol at distinct concentrations depending on the neurons lacking Fur1 and the differential rescue with the atypical clozapine, but not risperidone, argue that the drugs address particular spatially restricted receptors and also argue against generalized, nonspecific ameliorative effects of antipsychotics on *Drosophila* footshock habituation.

Discussion

Endophenotypes are fundamental observable symptoms that characterize and differentiate disease from normal behaviors. These are necessary simplifications to define and understand the genetic contribution to complex psychiatric illnesses, including schizophrenia. Deficient habituation is linked to and is considered an endophenotype of the disease (Williams et al., 2013; McDiarmid et al., 2017; Avery et al., 2019; Heinze et al., 2021). We demonstrate that the loss of *Drosophila* Fur1 specifically from adult α'/β' and γ MBNs results in robust deficits in footshock habituation. Significantly, the deficient footshock habituation facilitation is reversible with low-nanomolar concentrations of haloperidol and clozapine, drugs used to treat schizophrenic patients. Our collective evidence validates association studies linking variants in the human Furin gene to schizophrenia (Fromer et al., 2016, Christensen and Børglum, 2019; Schrode et al., 2019) and shows that deficient footshock habituation conforms to the criteria (Dwyer, 2018) and is a *Drosophila* protophenotype for the disease.

A

Receptor	Type	α′/β′	γ	Function	Predicted Fur site
GABA-B-R1	GABA		•	Inhibitory	
GABA-B-R2			•	Inhibitory	•
Rdl		•	•	Inhibitory	
Lcch3			•	Inhibitory	
Dop1R1	Dopamine	•	•	Excitatory	
Dop1R2		•	•	Excitatory	
Dop2R		•	•	Inhibitory	
DopEcR		•	•	Excitatory	
5-HT1A	Serotonin	•	•	Inhibitory	
5-HT1B			•	Inhibitory	•
Octbeta1R	Octopamine	•	•	Inhibitory	
CG18208 (Octalpha2R)			•	Inhibitory	•

B

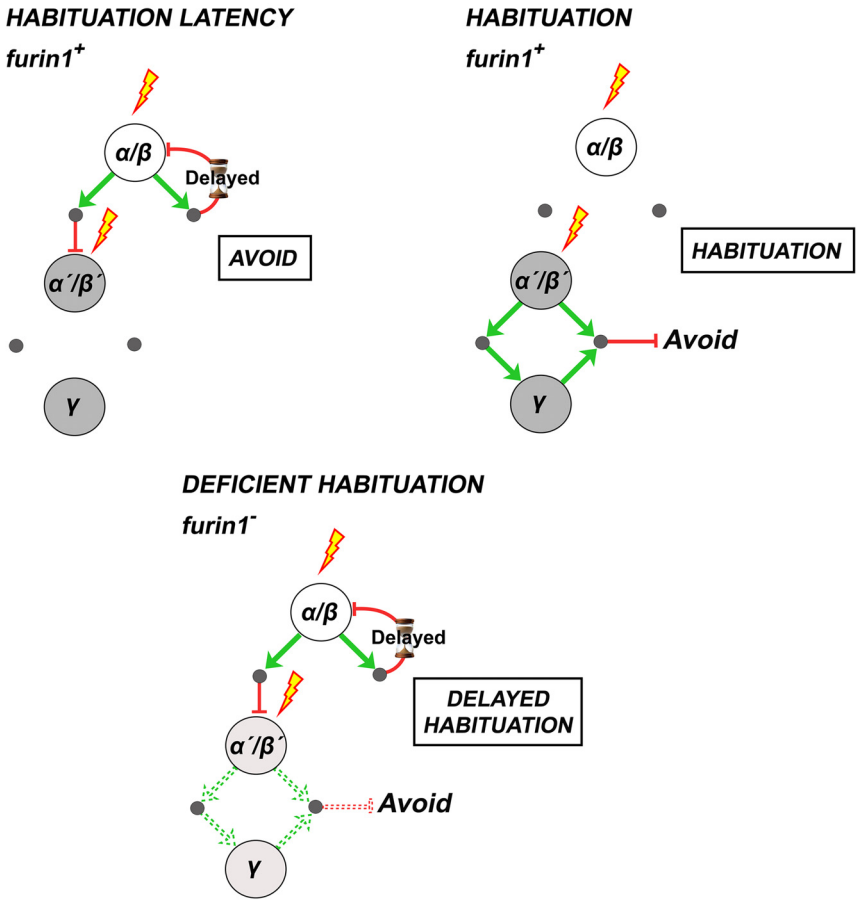

Figure 6. Footshock habituation model. ***A***, Summary of the receptors expressed in the indicated MBNs (Aso et al., 2019), their function, and predicted Furin cleavage sites. ***B***, The proposed model for *Drosophila* footshock habituation latency, habituation facilitation, and how Fur1 attenuation affects these processes are outlined. Incoming stimuli to α/β and α'/β' neurons are represented by the "thunderbolt" symbol. Large white circles indicate the MBNs in which Fur1 expression is not necessary for latency or habituation, while large gray circles indicate MBNs requiring Fur1 for the outlined processes. The large light gray circles denote Fur1-devoid MBNs. The small gray circles represent MBONs. The green arrows represent excitatory neurotransmission, and the red lines inhibitory neurotransmission. The dashed arrows and lines indicate reduced or inefficient excitatory or inhibitory neurotransmission.

The MBs have also been implicated in olfactory habituation latency, but are dispensable for habituation facilitation (Semelidou et al., 2018), in this paradigm. However, they are essential for habituation to ethanol vapor-induced startle (Cho et al., 2004) and for olfactory habituation in larvae (Hamid et al., 2021). Importantly, *fur1* mutants do not present olfactory habituation defects (Fig. 1*I*,*J*), suggesting that the protein is not involved in receiving or processing the largely cholinergic excitatory signals engaged in relaying olfactory information to the MBs (Amin and Lin, 2019). Although we did not investigate the role of Fur1 in larval olfactory or ethanol habituation in adults, our data indicate that the protein is engaged specifically in mechanisms underlying habituation to recurrent footshocks. This in turn indicates that MBNs use distinct molecular and circuitry engagement mechanisms to evaluate and respond to distinct stimuli.

Normal latency and habituation to the recurrent footshock stimuli are likely a network property requiring balanced excitatory and inhibitory signals (Glanzman, 2009; Rankin et al., 2009; Ramaswami, 2014). Attenuation of footshock avoidance underlying the habituated response is likely because of direct or indirect neurotransmission from MB output neurons (MBONs) to potentiate inhibition of stimulus avoidance (Ramaswami, 2014). We demonstrate that α'/β' neurons are necessary and sufficient, but neurotransmission from γ neurons is also required for habituation to recurrent footshocks. TANGO (Talay et al., 2017) was used to probe whether γ neurons synapse with their α'/β' counterparts, but, in agreement with connectome data (Li et al., 2020), such connections were not apparent (Fig. 5). Curiously however, a subset of dorsal β' neurons appears postsynaptic to α' and some β', while a more restricted subset of dorsal γ neurons appears postsynaptic to other γ neurons.

Alternatively, signals from α'/β' to γ neurons are required to drive the habituated response. In support of the notion that γ neurons are directly involved in driving the habituated response, compartments formed within γ neurons by the dendrites of afferent MBONs are known to drive approach and avoidance behaviors (Falsenberg, 2021). This agrees with our data that silencing neurotransmission from these neurons abrogates habituation (Fig. 2*G*). In addition, MBONs whose dendrites arborize both in γ and β' neurons have been described (Aso et al., 2014), suggesting that concurrent neurotransmission from β' and γ neurons drives habituation. This synergy scenario is supported by prior data (Roussou et al., 2019) and ones herein (Fig. 2*G*) that synaptic silencing of either α'/β' or γ neurons results in defective habituation.

Based on prior and current results (Acevedo et al., 2007; Roussou et al., 2019), we propose a model of this network,

currently under investigation. It posits that footshock stimuli may reach both α/β and α'/β' MBNs. However, neurotransmission from α/β neurons most likely indirectly, via MBONs (Aso et al., 2014), drives toward inhibition the activity of α'/β' neurons. Inhibition of α'/β' MBN activation does not alter the default response to the stimulus, which we posit is avoidance (Acevedo et al., 2007) and is manifested as latency to habituate (Fig. 6*B*). We suggest that α/β neurons concurrently signal to another inhibitory MBON, which we propose to have high activation threshold requiring multiple stimuli to depolarize, which is manifested as delayed activation relative to the incoming stimulus. This MBON impinges back on the α/β neurons (Aso et al., 2014) and inhibits their activity, effectively ending the latency period. Inhibition of α/β activity relieves the α'/β' inhibition shifting the balance to excitation, which results in γ MBN activation. We suggest that coordinated neurotransmission from α'/β' and γ to downstream inhibitory circuits results in attenuated avoidance of the stimuli manifested as habituation to footshock (Fig. 6*B*).

In the model presented in Figure 6*B*, α'/β' neurons receive the excitatory signal and relay the excitation to γ neurons, but their joint activity is required for habituation. This requirement for Fur1 within α'/β' neurons to receive activating signals and indirectly relay them to γ neurons is likely reflected in their necessary and sufficient role for habituation. Because γ neurons cannot be activated without signals from α'/β'neurons, Fur1 expression therein is likely important for their activation, but that depends on signals from their α'/β' counterparts deeming them necessary, but not sufficient, to drive habituation.

How does reduction of Fur1 within α'/β' and γ neurons result in prolonged latency manifested as delayed habituation (Fig. 1*C*,*D*,*F*)? The protein is typically located in the Trans-Golgi Network (TGN), where it is thought to cleave proprotein substrates, but also to traffic to the cytoplasm in vesicles, and it is even active on the cell surface where it is known to cleave substrates such as the anthrax toxin (Thomas, 2002). Hence, Furin may be involved in the maturation of excitatory aminergic receptors in a manner akin to its role in BDNF maturation (Chen et al., 2015). Although the predicted Furin cleavage consensus motif Arg-X-Lys/Arg-Arg (R-X-K/R-R; Thomas, 2002) is present in a number of aminergic and GABAergic receptors expressed in $\alpha'/\beta'$and γ neurons (Fig. 6*A*), it is currently unknown whether they are actually used, especially sites that fall within transmembrane or extracellular domains. However, evidence that activated receptor levels (Cheng and Filardo, 2012; Abdullah et al., 2016) or activity (Shioda et al., 2017) are regulated via the TGN suggest the possibility that Furin could in principle be involved in regulating receptor levels in α'/β' and γ neurons. In fact, $GABA_A$ receptor levels have been reported regulated by Furin levels in mice (Yang et al., 2018) and trafficking of the D_2 dopamine receptor depends on Furin activity (Blagotinšek Cokan et al., 2020).

Therefore, as for BDNF, Furin could be involved in maturation of excitatory aminergic receptors within α'/β' and γ MBNs, or D_2 receptor trafficking and its attenuation therein would reduce their levels. In this case, on relief of the α/β-mediated inhibition, the impact of incoming excitatory signals would be reduced in mutant α'/β' neurons impairing the shift toward excitation and neurotransmission to downstream circuits, resulting in delayed habituation. Reception of the α/β-originating inhibitory signals would not be affected as it would have precipitated premature habituation, which was not observed (Fig. 1*G*,*H*).

In this scenario, the antipsychotics are likely to reverse the habituation deficit by antagonizing receptors on α'/β' neurons receiving the α/β-mediated inhibitory signals, thus facilitating α'/β' excitation and activation of downstream habituation-mediating circuits. Alternatively, these drugs could act as agonists of excitatory receptors, whose reduced levels in mutant α'/β' neurons would perceive excitatory signals inefficiently. This would help shift the excitatory/inhibitory balance in α'/β' neurons toward excitation resulting in afferent signals driving habituation. The importance of the excitation/inhibition balance within neuronal circuits is underlined by reports that the excitatory HTR2A receptor is upregulated in schizophrenic patients (Greenwood et al., 2011; Morozova et al., 2019). Although the *Drosophila* ortholog (5-HT2A) is not expressed in α'/β' and γ MBNs, our model predicts that its overexpression therein may shift the balance and result in habituation defects, a hypothesis currently under consideration.

The multiple potential targets and modes of action of the antipsychotics used do not enable an unequivocal determination of their mechanism of action in the fly. However, overexpression or attenuation of their predicted target receptors within α'/β' and/or γ neurons that result in drug-reversible defective footshock habituation should enable elucidation of this critical question. However, establishing that attenuation of Fur1 in *Drosophila* yields a disease protophenotype, enables systematic, hypothesis-driven investigations of the molecular mechanisms underlying its loss, likely also perturbed in the human disease. Participants in these molecular pathways will probably be identified as disease-linked loci by extant or future GWAS studies. The genetic facility of *Drosophila* and its broad behavioral repertoire provide a system to efficiently validate GWAS-indicated schizophrenia loci, explore the mode of action of current antipsychotics, inform relevant research in extant mouse models (Nomura et al., 2017), and lead to the generation of new ones. This synergy will likely facilitate targeted translational approaches toward the development of more endophenotype/symptom-specific ameliorative drugs and better understanding of this complex disease.

References

Abdullah N, Beg M, Soares D, Dittman J, McGraw T (2016) Downregulation of a GPCR by β-Arrestin2-mediated switch from an endosomal to a TGN recycling pathway. Cell Rep 17:2966–2978.

Acevedo SF, Froudarakis EI, Kanellopoulos A, Skoulakis EM (2007) Protection from premature habituation requires functional mushroom bodies in Drosophila. Learn Mem 14:376–384.

Amin H, Lin A (2019) Neuronal mechanisms underlying innate and learned olfactory processing in Drosophila. Curr Opin Insect Sci 36:9–17.

Aso Y, Hattori D, Yu Y, Johnston RM, Iyer NA, Ngo TT, Dionne H, Abbott LF, Axel R, Tanimoto H, Rubin GM (2014) The neuronal architecture of the mushroom body provides a logic for associative learning. Elife 3:e04577.

Aso Y, Ray R, Long X, Bushey D, Cichewicz K, Ngo T, Sharp B, Christoforou C, Hu A, Lemire A, Tillberg P, Hirsh J, Litwin-Kumar A, Rubin G (2019) Nitric oxide acts as a cotransmitter in a subset of dopaminergic neurons to diversify memory dynamics. Elife 8:e49257.

Avery SN, McHugo M, Armstrong K, Blackford JU, Woodward ND, Heckers S (2019) Disrupted habituation in the early stage of psychosis. Biol Psychiatry Cogn Neurosci Neuroimaging 4:1004–1012.

Blagotinšek Cokan K, Mavri M, Rutland C, Glišić S, Senćanski M, Vrecl M, Kubale V (2020) Critical impact of different conserved endoplasmic retention motifs and dopamine receptor interacting proteins (DRIPs) on intracellular localization and trafficking of the D2 dopamine receptor (D2-R) isoforms. Biomolecules 10:1355.

Chen Y, Zhang J, Deng M (2015) Furin mediates brain-derived neurotrophic factor upregulation in cultured rat astrocytes exposed to oxygen-glucose deprivation. J Neurosci Res 93:189–194.

Cheng S, Filardo E (2012) Trans-Golgi Network (TGN) as a regulatory node for β1-adrenergic receptor (β1AR) down-modulation and recycling. J Biol Chem 287:14178–14191.

Cho W, Heberlein U, Wolf F (2004) Habituation of an odorant-induced startle response in Drosophila. Genes Brain Behav 3:127–137.
Christensen JH, Børglum AD (2019) Modeling the cooperativity of schizophrenia risk genes. Nat Genet 51:1434–1436.
Dwyer DS (2018) Crossing the worm-brain barrier by using Caenorhabditis elegans to explore fundamentals of human psychiatric illness. Mol Neuropsychiatry 3:170–179.
Dwyer DS, Awatramani P, Thakur R, Seeni R, Aamodt E (2015) Social feeding in Caenorhabditis elegans is modulated by antipsychotic drugs and calmodulin and may serve as a protophenotype for asociality. Neuropharmacology 92:56–62.
Falsenberg J (2021) Changing memories on the fly: the neural circuits of memory re-evaluation in Drosophila melanogaster. Curr Opin Neurobiol 67:190–198.
Fromer M, et al. (2016) Gene expression elucidates functional impact of polygenic risk for schizophrenia. Nat Neurosci 19:1442–1453.
Georganta E, Moressis A, Skoulakis E (2021) Associative learning requires neurofibromin to modulate GABAergic inputs to *Drosophila* mushroom bodies. J Neurosci 41:5274–5286.
Glanzman DL (2009) Habituation in Aplysia: the Cheshire cat of neurobiology. Neurobiol. Learn. Mem 92:147–154.
Gottesman I, Gould T (2003) The endophenotype concept in psychiatry: etymology and strategic intentions. Am J Psychiatry 160:636–645.
Greenwood T, et al. (2011) Analysis of 94 candidate genes and 12 endophenotypes for schizophrenia from the Consortium on the Genetics of Schizophrenia. Am J Psychiatry 168:930–946.
Hamid R, Sant H, Kulkarni M (2021) Choline Transporter regulates olfactory habituation via a neuronal triad of excitatory, inhibitory and mushroom body neurons. PLoS Genet 17:e1009938.
Heinze K, Barron H, Howes E, Ramaswami M, Broome M (2021) Impaired inhibitory processing: a new therapeutic target for autism and psychosis? Br J Psychiatry 218:295–298.
Insel T, Cuthbert B, Garvey M, Heinssen R, Pine D, Quinn K, Sanislow C, Wang P (2010) Research Domain Criteria (RDoC): toward a new classification framework for research on mental disorders. Am J Psychiatry 167:748–751.
Jenett A, et al. (2012) A GAL4-driver line resource for Drosophila neurobiology. Cell Rep 2:991–1001.
Kapur S, Mamo D (2003) Half a century of antipsychotics and still a central role for dopamine D2 receptors. Prog Neuropsychopharmacol Biol Psychiatry 27:1081–1090.
Kasap M, Rajani V, Rajani J, Dwyer DS (2018) Surprising conservation of schizophrenia risk genes in lower organisms reflects their essential function and the evolution of genetic liability. Schizophr Res 202:120–128.
Kepler L, McDiarmid T, Rankin C (2020) Habituation in high-throughput genetic model organisms as a tool to investigate the mechanisms of neurodevelopmental disorders. Neurobiol Learn Mem 171:107208.
Kitamoto T (2001) Conditional modification of behavior in Drosophila by targeted expression of a temperature-sensitive shibire allele in defined neurons. J Neurobiol 47:81–92.
Kotoula V, Moressis A, Semelidou O, Skoulakis E (2017) Drk-mediated signaling to Rho kinase is required for anesthesia-resistant memory in Drosophila. Proc Natl Acad Sci U|S|A 114:10984–10989.
Li F, et al. (2020) The connectome of the adult Drosophila mushroom body provides insights into function. Elife 9:e62576.
McDiarmid TA, Bernardos AC, Rankin CH (2017) Habituation is altered in neuropsychiatric disorders—a comprehensive review with recommendations for experimental design and analysis. Neurosci Biobehav Rev 80:286–305.
McGuire SE, Mao Z, Davis RL (2004) Spatiotemporal gene expression targeting with the TARGET and gene-switch systems in Drosophila. Sci STKE 2004:pl6.
Meincke U, Light GA, Geyer MA, Braff DL, Gouzoulis-Mayfrank E (2004) Sensitization and habituation of the acoustic startle reflex in patients with schizophrenia. Psychiatry Res 126:51–61.
Meyer-Lindenberg A, Weinberger D (2006) Intermediate phenotypes and genetic mechanisms of psychiatric disorders. Nat Rev Neurosci 7:818–827.
Modi M, Shuai Y, Turner G (2020) The Drosophila mushroom body: from architecture to algorithm in a learning circuit. Annu Rev Neurosci 43:465–484.
Morozova A, Zorkina Y, Pavlov K, Pavlova O, Storozheva Z, Zubkov E, Zakharova N, Karpenko O, Reznik A, Chekhonin V, Kostyuk G (2019) Association of rs4680 *COMT*, rs6280 *DRD3*, and rs7322347 *5HT2A* with clinical features of youth-onset schizophrenia. Front Psychiatry 10:830.
Naheed M, Green B (2001) Focus on clozapine. Curr Med Res Opin 17:223–229.
Nomura J, Kannan G, Takumi T (2017) Rodent models of genetic and chromosomal variations in psychiatric disorders. Psychiatry Clin Neurosci 71:508–517.
Papanikolopoulou K, Roussou I, Gouzi J, Samiotaki M, Panayotou G, Turin L, Skoulakis E (2019) *Drosophila* tau negatively regulates translation and olfactory long-term memory, but facilitates footshock habituation and cytoskeletal homeostasis. J Neurosci 39:8315–8329.
Patel KR, Cherian J, Gohil K, Atkinson D (2014) Schizophrenia: overview and treatment options. P T 39:638–645.
Ramaswami M (2014) Network plasticity in adaptive filtering and behavioral habituation. Neuron 82:1216–1229.
Rankin CH, Abrams T, Barry RJ, Bhatnagar S, Clayton DF, Colombo J, Coppola G, Geyer MA, Glanzman DL, Marsland S, McSweeney FK, Wilson DA, Wu CF, Thompson RF (2009) Habituation revisited: an updated and revised description of the behavioral characteristics of habituation. Neurobiol Learn Mem 92:135–138.
Richard EA, Khlestova E, Nanu R, Lisman JE (2017) Potential synergistic action of 19 schizophrenia risk genes in the thalamus. Schizophr Res 180:64–69.
Ripke S, et al (2014) Biological insights from 108 schizophrenia-associated genetic loci. Nature 511:421–427.
Roebroek AJ, Creemers JW, Pauli IG, Bogaert T, Van de Ven WJ (1993) Generation of structural and functional diversity in furin-like proteins in Drosophila melanogaster by alternative splicing of the Dfur1 gene. EMBO J 12:1853–1870.
Roussou IG, Papanikolopoulou K, Savakis C, Skoulakis EMC (2019) *Drosophila* Bruton's tyrosine kinase regulates habituation latency and facilitation in distinct mushroom body neurons. J Neurosci 39:8730–8743.
Schrode N, et al. (2019) Synergistic effects of common schizophrenia risk variants. Nat Genet 51:1475–1485.
Semelidou O, Acevedo SF, Skoulakis EM (2018) Temporally specific engagement of distinct neuronal circuits regulating olfactory habituation in Drosophila. Elife 7:e39569.
Sharma P, Keane J, O'Kane CJ, Asztalos Z (2009) Automated measurement of Drosophila jump reflex habituation and its use for mutant screening. J Neurosci Methods 182:43–48.
Shioda N, Yabuki Y, Wang Y, Uchigashima M, Hikida T, Sasaoka T, Mori H, Watanabe M, Sasahara M, Fukunaga K (2017) Endocytosis following dopamine D2 receptor activation is critical for neuronal activity and dendritic spine formation via Rabex-5/PDGFRβ signaling in striatopallidal medium spiny neurons. Mol Psychiatry 22:1205–1222.
Shyu WH, Chiu TH, Chiang MH, Cheng YC, Tsai YL, Fu TF, Wu T, Wu CL (2017) Neural circuits for long-term water-reward memory processing in thirsty Drosophila. Nat Commun 8:15230.
Sokal R, Rohlf F (2012) Biometry: the principles and practice of statistics in biological research, Ed 2. San Francisco: WH Freeman.
Talay M, Richman EB, Snell NJ, Hartmann GG, Fisher JD, Sorkaç A, Santoyo JF, Chou-Freed C, Nair N, Johnson M, Szymanski JR, Barnea G (2017) Transsynaptic mapping of second-order taste neurons in flies by trans-Tango. Neuron 96:783–795.e4.
Thomas G (2002) Furin at the cutting edge: from protein traffic to embryogenesis and disease. Nat Rev Mol Cell Biol 3:753–766.
van Os J, Kapur S (2009) Schizophrenia. Lancet 374:635–645.
Williams LE, Blackford JU, Luksik A, Gauthier I, Heckers S (2013) Reduced habituation in patients with schizophrenia. Schizophr Res 151:124–132.
Yang Y, He M, Tian X, Guo Y, Liu F, Li Y, Zhang H, Lu X, Xu D, Zhou R, Ma Y, Wang W, Chen G, Hu Y, Wang X (2018) Transgenic overexpression of furin increases epileptic susceptibility. Cell Death Dis 9:1058.